Doctoral dissertation

Singlet Oxygen from Endoperoxide Initiates an Intracellular ROS Release in HaCaT Keratinocytes

Elshafei Maryam Emad

ID: 1414192501

Under the supervision of Professor Hiroshi Ichikawa

Graduate School of Life and Medical Sciences

Doshisha University

2022

Abstract

Singlet oxygen ($^1O_2$) is a selective intermediate reactive oxygen species (ROS) generated naturally in biological systems by light- and non-light mediated processes. Although $^1O_2$ plays an important role in cell signalling and in maintaining homeostasis, it can be toxic due to its ability to diffuse across considerable distances. Several *in vitro* studies have investigated the pathways by which $^1O_2$ mediates oxidation of biological molecules and potential pathogenesis. However, understanding if and how singlet oxygen exerts cell injury through the production of subsequent ROS remains unexplored. To study this, a hydrophobic endoperoxide (EP) was utilised as a source of $^1O_2$. Endoperoxides are reagents that quantitatively generates singlet oxygen in solution at 35 °C by thermal decomposition. The chemiluminescence and cell viability assay data revealed that $^1O_2$ stimulated a secondary intracellular ROS production in a very short time. To determine the source of these ROS with EP exposure, cells were treated with inhibitors targeting NADPH oxidases and platelet activating factor receptors. The results showed that addition of the platelet activating factor receptor (PAF-R) antagonist, WEB2086, alleviated cell injury and hydrogen peroxide levels following endoperoxide stimulation. Furthermore, intramitochondrial singlet oxygen was visualised using fluorescent dye and confocal microscopy, revealing a secondary singlet oxygen production from the mitochondria following EP exposure. This PAF-R and mitochondrial activation for ROS production could potentially be calcium sensitive as the intracellular calcium assay data demonstrated that EP stimulated a rise in calcium levels.

Table of contents

1. Introduction

Singlet oxygen ($^1O_2$) is a naturally occurring reactive oxygen species (ROS) that plays important roles in biological systems. Under normal conditions (i.e., oxidative eustress), this ROS functions as a secondary messenger during cell signalling (Ray, Huang and Tsuji, 2012), and as an antimicrobial in immune response (Ogilby, 2010). However, singlet oxygen readily oxidizes several biological molecules, particularly proteins, DNA, and lipids. Therefore, when its production rises above homeostatic levels, it leads to disease pathogenesis and cell injury (i.e., oxidative distress) (Devasagayam and Kamat, 2002; Agnez-lima *et al.*, 2012).

Singlet oxygen functions as an intermediate ROS in biological systems, since it can diffuse across considerable distances (Hrycay and Bandiera, 2015), and processes involving its production readily lead to secondary reactive by-products such as lipid peroxidation (Ouedraogo and Redmond, 2003; Ogilby, 2010). Although several *in vitro* studies have been conducted to understand the functions of singlet oxygen in the cell, none of them have addressed its cell injury pathway via the ROS production cascade. Consequently, the mechanism by which this phenomenon occurs and the specific pathways involved remain unknown.

Photochemical reactions involving photosensitizers are a commonly used source of this ROS. This can be done through either type I or type II photosensitised generation reactions. In type I reactions, the excited triplet sensitizer reacts directly with the substrate to produce a radical or radical-ion in both the sensitizer and the substrate following the absorption of UV light by chromophores. Whereas in type II reactions, the excited triplet

sensitizer (e.g., methylene blue) first interacts with ground-state molecular oxygen ($^3O_2$) to produce $^1O_2$, which can be used to specifically investigate the roles of $^1O_2$ in cellular systems. This method, however, is not ideal in exclusively studying the functions of singlet oxygen as it simultaneously produces other ROS (Nagaoka *et al.*, 2005). According to Davies (2003), singlet oxygen can be also be generated by a number of biologically relevant processes that are non-light dependent (i.e., 'dark' reactions). These processes include generation by stimulated cells in immune response, and generation via the reaction of hydrogen peroxide with hypochlorous acid and reactive nitrogen species. Therefore, to simulate these processes *in vitro* using a more specific and easily utilised source, chemical generation of singlet oxygen in solution by thermal decomposition of endoperoxides (EPs) was used.

EP is a reagent that is widely used in Japan for singlet oxygen absorption capacity assays of antioxidants (Ouchi *et al.*, 2010), and previously developed as a useful tool for singlet oxygen stimulation in biological studies (Pierlo *et al.*, 2000). Therefore, this study investigated the effects of singlet oxygen from EP as a biological stimulus on the intracellular generation of ROS as well as the possible pathways associated with it.

2. Materials and Methods

I. Materials

I-1 Cell culture

Human epidermal keratinocytes (HaCaT cells, CLS order no. 30049; lot number 300493-315SF) were used in all experiments carried out in this study. The cells were cultured in Dulbecco's Modified Eagle's Medium – high glucose (D6429-500 mL, 4500 mg/L glucose in D-MEM; Sigma-Aldrich, St. Louis, MO), Fetal Bovine Serum (FBS) (171012-500 mL, Nichirei Biosciences, Tokyo) 10%, antibiotic antimycotic solution (10,000 unit/mL penicillin G, 10 mg/mL streptomycin sulphate, 25 μg/mL amphotericin B; Sigma-Aldrich, MO, US) was added to 1%. Trypsin-EDTA (0.05%), phenol red (25300054, Gibco) was used to passage cells. Washing was done using 9.6 g of Dulbecco's PBS (-) (05913, Nissui Pharmaceutical Co., Ltd., Japan) dissolved in 1 L of distilled water and sterilised by autoclaving.

I-2 Endoperoxide (EP)

I-2.1 EP

Endoperoxide (50 mg, Waken B. tech, Kyoto, Japan) was prepared by dissolving the powder in 0.1% dimethyl sulfoxide (DMSO; 500ml, Fuji Film Wako Pure Chemical Industries, Ltd., Osaka, Japan).

I-2.2 Inactive EP (used as control)

Following I-2.1, the solution of 1 mM EP was maintained at 37 °C in an incubator with a humidified atmosphere of 5% CO_2 (Thermo Fisher Scientific) for 24 hours.

I-3 Chemiluminescence (CL) reagents

I-3.1 MCLA

1 µM MCLA (2-methyl-6-(p-methoxyphenyl)-3, 7 -dihydroimidazole (1, 2-1) pyrazin-3-one) was prepared by dissolving 0.29 mg MCLA (TCI, Tokyo, Japan) in 1 mL distilled water to make a concentration of 100 µM. The solution was then aliquoted into 100 µL and added to 1.5 mL amber Eppendorf tubes (i.e., light protected) then stored at -20 °C. Prior to use, 900 µL of distilled water was added to the tube to further dilute the MCLA reagent to final concentration 1 µM.

I-3.2 L-012

800 µL of distilled water was added to 200 µL of the luminol L-012 (8-Amino-5-chloro-2,3-dihydro-7-phenylpyrido [3,4- d] pyridazine-1,4-dione monosodium salt; Fujifilm Wako Pure Chemicals, Japan) to dilute the 50 µM reagent to 1 µM final concentration.

I-4 ROS scavengers, antagonists, and inhibitors

I-4.1 Sodium azide (NaN₃)

Sodium azide is a scavenger of singlet oxygen ($^1O_2$). The powder (NaN$_3$, molecular weight 65.01; 197-11091, Fujifilm Wako Pure Chemicals, Osaka, Japan) was dissolved in distilled water to prepare a concentration of 100 mM. Zero medium (MFG No. cf0926a0 – 500 mL, without glucose, sodium bicarbonate, Penicillin/Streptomycin, HEPES; CSTI Custom medium, Cell Science and Technology Inst., Inc.), or Hank's balanced salt solution (HBSS DLR7002, with 1% antibiotic antimycotic solution; Fujifilm Wako Pure Chemicals, Osaka, Japan) were then used to further dilute the reagent to a final concentration of 1 mM.

I-4.2 L-Histidine (His)

L-Histidine is a potent scavenger of $^1O_2$. 0.78 mg of L-Histidine (Fujifilm Wako Pure Chemical Industries, Ltd., Osaka, Japan) was dissolved to a final concentration of 1 mM in 5 mL Zero medium (MFG No. cf0926a0 – 500 mL, without glucose, sodium bicarbonate, Penicillin/Streptomycin, HEPES; CSTI Custom medium, Cell Science and Technology Inst., Inc.)

I-4.3 Superoxide Dismutase (SOD)

SOD is an enzyme that catalyzes the dismutation of extracellular superoxide anion ($O_2^{\cdot-}$). SOD powder (NIPPON KAYAKU CO. LTD. NK341) was dissolved in distilled water to a final concentration of 10,000 U / mL, aliquoted, and stored at 4 ° C. The solution was then diluted 10-fold with Zero medium or HBSS (-) to 1,000 U / mL.

I-4.4 Catalase (CAT)

Catalase is an enzyme that catalyzes the decomposition of hydrogen peroxide (H_2O_2) to water and oxygen. Catalase (9001-05-2, Fujifilm Wako Pure Chemical Industries, Ltd., Osaka, Japan) with an initial concentration of 30,000 U/mL was diluted 30-fold using the similar to I-4.1 to a final concentration of 1,000 U/mL.

I-4.5 MnTMPyP

MnTMPyP is a cell-permeable SOD mimetic. 0.143 mg of MnTMPyP (MnTMPyP-Calbiochem: 475872, Merck KGaA, Germany) was dissolved in 10 mL Zero medium or HBSS (-) to a final concentration of 10 μM. The remaining solution was aliquoted and stored at -20°C (i.e., protected from light and moisture).

I-4.6 Dimethyl sulfoxide (DMSO)

DMSO is a scavenger of hydroxy radicals ($\cdot$ OH). The DMSO stock solution (DMSO: Fujifilm Wako Pure Chemical Industries, Ltd., Osaka, Japan) is diluted with Zero medium to 1% and stored at 4°C. When used, the DMSO solution was further diluted to a final concentration of 0.1% using Zero medium.

I-4.7 Apafant (WEB2086)

WEB 2086 is a potent, selective platelet activating factor (PAF) receptor antagonist. WEB 2086 (SML 0238-5MG, Sigma-Aldrich, MO, US) was prepared by dissolving 1 mg in 220 μL of DMSO. 1.98 mL of PBS (-) was then added to reach a final concentration of 10 mM (and DMSO concentration of 10%). When used, the solution was diluted to 100-fold using Zero medium or HBSS (-) to a final concentration of 10 μM (i.e., final concentration of DMSO is 0.1%).

I-4.8 Diphenyleneiodonium chloride (DPI)

DPI is a widely used NADPH oxidase and DUOX inhibitor. 5 mg of DPI (CAY-81050, Funakoshi, Tokyo, Japan) was dissolved in 1.59 mL of DMSO to prepare an initial concentration of 10 mM. The solution was then diluted accordingly using HBSS (-) or medium.

I-5 Electron transport chain (ETC) inhibitors

I.5.1 Rotenone (RT)

Rotenone is an inhibitor of complex 1 (NADH dehydrogenase) in the mitochondrial electron transport chain. 0.3944 mg rotenone (M5296, Fujifilm Wako Pure Chemical Industries, Ltd., Osaka, Japan) was dissolved in 1 mL DMSO to prepare a concentration of 1 mM. The solution was then diluted to 50 µM using distilled water, and diluted 10-fold with DMEM to a final concentration of 5 µM.

I.5.2 Antimycin A (AA)

Antimycin A is an inhibitor of the ubiquinone cycle of complex III (cytochrome c reductase) of the mitochondrial electron transport chain. 10 mg of AA (25911218, Fujifilm Wako Pure Chemical Industries, Ltd., Osaka, Japan) was dissolved in 182 mL of DMSO to a make a concentration of 100 mM. Further dilution was done with DMSO to 25 mM, and adjusted to 250 µM using distilled water. A final concentration of 25 µM was then prepared by diluting the solution 10-fold with DMEM.

I.5.3 Thenoyltrifluoroacetone (TTFA)

TTFA is an inhibitor of complex II (succinate dehydrogenase) of the mitochondrial electron transport chain. 22.22 g of TTFA (6754E, Funakoshi, Tokyo, Japan) was dissolved in 400 µL DMSO to an initial concentration of 250 mM. The solution was then diluted to 2.5 mM using distilled water, and diluted 10-fold with DMEM to a final concentration of 250 µM.

I-6 WST-8 reagent

To determine the number of viable cells, Water Soluble Tetrazolium salt (WST- 8), and a mixture of cell proliferation or cytotoxicity measurement reagent Cell Counting Kit-8 (CCK-8: 343-07623 Dojindo Chemical Laboratory, Kumamoto, Japan) was used with a mixture of FBS (10%) high glucose D-MEM. Measurement of absorbance was done using Thermo Scientific Varioskan Flash Multimode Reader (Cat. No. N06354, Thermo Fisher Scientific, US).

I-7 Red Hydrogen peroxide

Red Hydrogen Peroxide assay kit (ENZ-51004, Enzo Life Sciences) solution was used to measure hydrogen peroxide concentration in solution and cells. 1 mL of 20 mM hydrogen peroxide solution was first prepared by adding 977 µL of assay buffer and 22.7 µL of 3% hydrogen peroxide stabilized solution in an Eppendorf. 1 µM of the aforementioned solution was then diluted by assay buffer to make a standard of 10 µM. This standard was used to prepare the remaining standard concentrations: 0.01, 0.03, 0.1, 0.3, 1, and 3 µM by serial dilution. Finally, 50 µL stock red peroxidase, 200 µL stock 20 U/ mL peroxidase, and 4.75 mL KRB (for cells)/ assay buffer (no cells) were added to prepare the hydrogen peroxide reaction mixture. Fluorescence was measured using Perkin Elmer ARVO MX microplate reader.

I-8 Calcium Kit-II Fluo 4

Intracellular calcium levels were measured using Calcium Kit II Fluo-4 fluorescent probe (1- [2-Amino-5- (2,7-difluoro-6-acetoxymethoxy-3-oxo-9-xanthenyl) phenoxy] -2- (2-amino-5-methylphenoxy) ethane- N, N, N', N'-tetra acetic acid, tetra (acetoxymethyl) ester; Dojindo, Japan). The fluorescent reagent was prepared by dissolving the Fluo4-AM powder in 50 µL DMSO. The solution was then added to a mixture of 5 mL Quenching buffer, 500 µL Hanks' HEPES Buffer (10X), 160 µL Pluronic F-127, and 100 µL 250 mM Probenecid. Fluorescence was measured using Perkin Elmer ARVO MX microplate reader.

I-9 Fluorescent reagents and microscopy

I.9.1 Si-DMA

Si-DMA was used for mitochondrial singlet oxygen imaging. 2 µM of Si-DMA powder (CAS number: 1621598-01-3, Fujifilm Wako Pure Chemical Industries, Ltd., Osaka, Japan) was dissolved in 36 µL of DMSO to prepare a final concentration of 100 µM.

I.9.2 MitoBright LT Green

Used as a chemiluminescent probe for intramitochondrial singlet oxygen, commercially available 100 µM MitoBright LT Green (CAS number: 67-68-5, Fujifilm Wako Pure Chemical Industries, Ltd., Osaka, Japan) was diluted 500-fold using HBSS (-).

I.9.3 Fluorescent microscopy

Fluorescence was observed using Zen 3 LSM900 (Zeiss, Germany) confocal microscope, and Axio observer version 7.

II. Methods

II-1 HaCaT cell culture

HaCaT cells were cultured in a 10-cm dish (150464, Thermo) in D-MEM medium at 37 °C, 5% CO_2 incubator (Thermo Fisher Scientific). Following confluence, the culture solution was removed using an aspirator, and the dish was washed twice with 2 mL PBS (-). After removing PBS (-), 1 mL of Trypsin-EDTA (0.05%) and phenol red were added, and the dish was placed in an incubator for 5-10 minutes to release the cells. 5 mL of D-MEM medium was then added and the cell suspension was moved to a 50 mL Falcon tube (227261, Greiner) for centrifugation at 1,500 rpm, 20 °C. The supernatant was removed using an aspirator, the appropriate amount of D-MEM medium was added followed by mixing. Using a hemocytometer, the cell number was counted and a cell suspension of 15×10^5 cells/ dish was added to a fresh 10 cm dish. (8.0×10^5 cells/ dish for 6 cm dish). D-MEM medium was added so that the total volume becomes 10 mL after seeding (4 mL in a 6 cm dish). All dishes were then incubated for 48 hours for each passage.

II-2 WST-8 Assay

WST-8 Assay is a method used to quantitatively measure viable cells through cellular mitochondrial activity. In a 96-well plate (655180, Greiner), HaCaT cells were seeded at a concentration of 2.0×10^5 cells/ mL in 100 µL/ well and incubated for 24 hours. Following confluence, the culture solution was removed with a 200 µL micropipette and washed twice with 100 µL PBS (-). PBS (-) was then removed, and culture or stimulation was performed under the desired conditions. A mixed solution of Cell Counting Kit-8 reagent and FBS (10%) D-MEM medium (or Zero medium) at a ratio of 1:10 was prepared, and 100 µL of the solution was added to each well. Blanks were prepared by adding the same solution to wells without cells. The plate was then incubated for 30 minutes and the absorbance was measured at 450 nm.

II-3 MCLA and L-012 CL analysis

II-3.1 EP preparation

EP solution was prepared by dissolving the powder in DMSO to a final concentration of 1 mM (10 mM in chemiluminescence).

II-3.2 Cell sample preparation

For cell samples, HaCaT cells were cultured 48 hours prior until confluence and resuspended in KRB to make a solution with a cellular concentration of $7.0-9.0 \times 10^5$. Cells were treated with 10 µM of the ROS scavenger, MnTMPyP, for 10 minutes prior to washing and collection. Similarly, 2.5 µM DPI was added to cells for 2 minutes prior to CL analysis.

II-3.3 Measurement method

100 µL of the CL reagents MCLA or L-012, 50 µL of ROS scavengers, and 300 µL Krebs-Ringer Buffer (KRB) were added in a number 4 Eiken tube (Eiken Chemical Co., Ltd.), and measurement was initiated for 60 seconds. 50 µL of EP solution in 0.1 % DMSO was then added and measurement was completed for 1000 seconds. To measure cellular ROS,

II-3.4 Analysis

ROS generation was evaluated by area under the curve starting from 64 seconds (i.e., total emission following stimulation), and the peak-base value (maximum emission intensity), and represented as a bar graphs.

II-4 Cell viability assay following stimulation with singlet oxygen from EP, and the effect of ROS scavengers in improving viability

Cell culture was performed as stated in II-1 in a 96-well plate and the experimental method was then carried out similar to II-2 as WST-8 assay was employed. Stimulation was done using 1 mM EP as stated in I-3.1 with varying incubation times initially, with a final selected time of 1-hour for all experiments. Three different methods were implemented for ROS scavengers: pre-incubation, co-incubation, and post-incubation (**Figure 17**). Inactive EP (I-3.2) was used as a control in all experiments.

II-5 Determining safe concentration of DPI, and testing the relevance of Nox as a source of subsequent ROS

Cell culture was performed as previously stated, and the experimental method was then carried out similar to II-2 as WST-8 assay was employed. HaCaT cells were treated with DPI concentrations of varying concentrations for 2 minutes to determine safe concentration of the inhibitor to use. For stimulation, 1 mM EP was added to cells for one hour following 2.5 µM DPI pre-treatment in all cell viability experiments.

II-6 Hydrogen peroxide assay

Cells were seeded at a concentration of 2.0×10^5 cells/ mL in 100 µL/ well in a black 96 well plate (Thermo Fisher Scientific) overnight until confluence. The plate was washed using PBS (-), and cells were treated with ROS scavengers or DPI prior to 1 mM EP stimulation as previously mentioned in II-4 and II-5. The same method was used to measure hydrogen peroxide concentration in media only with EP stimulation. Following incubation, hydrogen peroxide reaction mixture (as prepared in I-7) was added to both standards and samples. The fluorescence intensity of the standards was then measured using a microplate reader at a wavelength of Ex570/ Em590 nm, and the standards curve equation was used to calculate the hydrogen peroxide concentration of the samples.

II-7 Intracellular calcium assay

HaCaT keratinocytes were seeded in a black 96 well plate overnight until confluence. The plate was then washed with PBS (-), and cells were stimulated by incubation with EP concentrations of 0, 50, 100, 500, and 1000 µM for one hour. Following EP stimulation, the plate was washed again and Calcium Kit II– Fluo 4 (as prepared in I-8) was subsequently added to the cells. Fluorescence intensity was then measured at a wavelength of 485/ 535 nm in a microplate reader. For groups with DPI pre-treatment, and WEB2086 groups, the samples were prepared according to II-5 and II-4 (co-incubation) respectively.

II-8 Real-time fluorescence imaging of EP-induced intramitochondrial singlet oxygen production

II-8.1 Sample preparation

HaCaT cells were seeded at a concentration of 3.0×10^5/ mL in a glass bottom petri dish (CELL view 35 x10 mm TC4 compartments 1.9 cm^2, E210346T, Greiner bio-one, Germany) and cultured in DMEM overnight until confluence. The dishes were then washed twice with HBSS (-), and the fluorescent reagents (as prepared in I-9.1 and I-9.2) were added for one hour.

II-8.2 Stimulation by EP

1 mM EP was prepared as previously mentioned, and activated by placing in a water bath at 37 °C for 10 minutes before adding to cell samples. The cells were then incubated with EP for 30 minutes, and imaging was subsequently observed using a confocal microscope. The negative controls, inactive EP and HBSS (-), were used and prepared similar to previous experiments.

II-8.3 Addition of ROS scavengers and inhibitors

All ROS scavengers and ETC inhibitors were prepared as previously mentioned in I-4 and I-5 respectively. The cells were treated with DPI and ETC inhibitors for only 2 minutes prior to EP stimulation, while the ROS scavengers were added concomitantly with stimulation for the full 30 minutes.

II-9 Statistical analysis

Statistical significance between groups was evaluated using Tukey HSD post-hoc test, and one way ANOVA. For significant difference, the risk rate was tested at 5% on both sides. All analyses were performed on IBM SPSS ver. 27 and Microsoft Excel 2016.

3. Results

I. Endoperoxide releases singlet oxygen in a dose-dependent manner. In order to determine the effective concentration of EP for this study, MCLA CL was employed to measure singlet oxygen release. The data (**Figure 1**) shows that singlet oxygen production increased dose-dependently from EP solutions prepared in 0.1% DMSO when measured for 1000 seconds.

II. ROS production from 1 mM endoperoxide is significantly increased in the presence of cells. In both MCLA and L-012 CL analysis data (**Figure 2**), ROS production rate was significantly higher in samples containing cells compared to those that did not.

III. Sustained intracellular superoxide and singlet oxygen production occurred following 1 mM endoperoxide exposure. In MCLA and L-012 CL analysis for detection of superoxide and singlet oxygen radicals (**Figure 3**), treatment with 10 mM sodium azide (NaN_3), 1000 U/ mL superoxide dismutase (SOD), and 10 µM of the cell-permeable SOD mimetic (MnTMPyP) significantly reduced the intracellular ROS production with 1 mM EP stimulation. In **Figure 4**, L-012 CL analysis failed to accurately measure hydrogen peroxide release from cells when treated with 1000 U/ mL catalase (CAT) and 10 µM WEB2086. However, alleviation is noted when compared to control.

IV. 1 mM endoperoxide stimulation lowered cell viability within one hour. Cell viability assay data for 1-, 3-, 6-, 9-, and 12-hours incubation with 1 mM EP solution reveals a significant reduction in viability when compared to the control group (**Figure 5**).

V. ROS scavengers targeting superoxide, singlet oxygen, and hydrogen peroxide improved cell viability. Pre-, co-, and post-incubation cell viability assay data demonstrate significant improvement in viability in groups treated with ROS scavengers; particularly those targeting singlet oxygen, intracellular superoxide, and intracellular hydrogen peroxide with EP stimulation (**Figure 6**).

VI. Determining safe concentration of the Nox inhibitor, diphenyleneiodonium chloride (DPI), to use. According to the WST-8 assay data, DPI was safe up to a concentration of 2.5 µM (**Figure 7**).

VII. NADPH oxidases are not a major source of intracellular ROS following endoperoxide exposure. Pre-treating cells with 2.5 µM of DPI did not cause a significant improvement in cell viability **(Figure 8A)** nor did it significantly reduce ROS production with 1 mM EP stimulation **(Figure 8B)**. Similarly, no significance was noted in the WST-8 nor MCLA CL analysis either when cells were treated with ROS scavengers targeting singlet oxygen and superoxide (**Figures 9 &10**).

VIII. Platelet activating factor receptor (PAF-R) pathway could be one of the main sources of ROS following endoperoxide stimulation. As stated earlier; in pre-, co-, and post-incubation cell viability assay data, the PAF-R antagonist, WEB2086, counteracted the cell injury caused by 1 mM EP (**Figure 6**). In addition, hydrogen peroxide assay data (**Figure 11B**), demonstrate a significant reduction in hydrogen peroxide concentration when cells were co-incubated with WEB2086 and EP.

IX. Endoperoxide causes a rise in intracellular calcium levels. This increase, however, was counteracted by blocking Nox and PAF-R. Intracellular calcium assay data revealed a steady, dose-dependent increase in intracellular calcium with EP (**Figure 12A**). Pre-treatment with DPI or co-incubation with the PAF-R antagonist, WEB2086, significantly countered the rise in intracellular calcium levels caused by 1 mM EP stimulation (**Figure 12B**).

X. Mitochondria are a source of subsequent intracellular singlet oxygen following 1 mM EP stimulation. In WST-8 assay, pre-treating the cells with electron transport chain (ETC) inhibitors rotenone (RT) and antimycin A (AA) at concentrations of 5 µM and 25 µM respectively, did not reveal significant improvement in viability with 1 mM EP stimulation (**Figure 13**B). However, a rise in intramitochondrial singlet oxygen is observed with EP exposure (vs controls) as depicted in Si-DMA imaging (**Figure 14**). Moreover, this increase was counteracted when cells were treated with ETC inhibitors (**Figure 15A**), WEB2086 (**Figure 15B**), and the ROS scavengers: MnTMPyP, NaN_3, His (**Figure 16**).

4. Discussion

Firstly, chemiluminescence (CL) assay was employed to determine an effective concentration of the EP. This method can detect ROS via oxidation reactions using specific CL probes or reagents. L-012 (a luminol derivative) and 2-methyl-6-(4-methoxyphenyl)-3,7- dihydroimidazole [1,2-a] pyrazin-3-one (MCLA) probes were selected, according to a previous study that extensively evaluated various CL reagents. This is because of their high sensitivity in detecting different ROS, specifically superoxide ($O_2^{\bullet-}$) and singlet oxygen radicals ($^1O_2$)(Yamaguchi *et al.*, 2010). Results using MCLA CL revealed a dose-dependent rise in singlet oxygen levels with EP stimulation, and a high detection in 1000 µM solution (i.e.,1 mM) **(Figure 1)**. The evaluation was performed for approximately 16 min, with a peak reading at approximately 8 min, followed by a steady decline. This shows that EP releases singlet oxygen for a short time (i.e., less than one hour), and is consistent with previous studies using 1-methylnaphthalene-4-propionate endoperoxide, which is hydrophobic and structurally similar to the EP used in this study (Otsu *et al.*, 2005).

Skin exposure to several extracellular stimuli such as toxins, ultraviolet radiation, and drugs, generates intracellular ROS in excessive quantities which lead to disease pathogenesis (Bickers and Athar, 2006). Interestingly, when samples containing cells were compared to those without in the MCLA and L-012 CL data, ROS detection was significantly higher in the cell group **(Figure 2)**. These data confirmed that cellular ROS production is possible in response to EP stimulation. Furthermore, CL is a sensitive method for ROS detection, but fails to detect normal intracellular ROS levels (Kim *et al.*, 2019). Therefore, the slight increase in the CL reading with cells may indicate an

excessive production of ROS. However, this production was not limited to $^1O_2$, $O_2^{\bullet-}$ was also detected according to the data containing scavengers targeting this ROS; namely superoxide dismutase (SOD) and the cell permeable SOD mimetic, MnTMPyP (**Figure 3**). Although the ROS released seemed to be predominantly singlet oxygen and superoxide, minute amounts of hydrogen peroxide were noted using L-012 (**Figure 4**).

To analyse the effect of ROS production on cell function and further confirm the CL findings, the water-soluble tetrazolium (WST)-8 kit was used. The results showed that 1 mM EP, which produced about 5.6×10^6 relative light units of singlet oxygen per second (RLU/sec) at maximum reading, significantly lowered cell viability after one hour of incubation (**Figure 5**). This finding supports the hypothesis that EP at this concentration is toxic to cells. Furthermore, treating the cells with scavengers targeting intracellular superoxide (MnTMPyP), hydrogen peroxide (WEB2086), and singlet oxygen (His and NaN$_3$) improved viability (**Figure 6A−B**), which was consistent with the CL data. Post-incubation data especially upholds the theory that exposure to EP resulted in an intracellular ROS response, as the scavengers were still effective even after removal of the stimulant (**Figure 6C**). Additionally, when cells were treated with scavengers that exclusively neutralize extracellular superoxide and hydrogen peroxide, cell viability remained unchanged. Yet, it is still unclear whether this effect is due to the oxidation of biological molecules or the consequent ROS production caused by singlet oxygen.

Next, it is important to identify the source of intracellular ROS in response to singlet oxygen stimulation. HaCaT keratinocytes express the enzymes, NADPH oxidases (Nox), particularly Nox-1, 2, 4 (Chamulitrat *et al.*, 2004) and 5 (Benedyk *et al.*, 2007), at the mRNA level with different subcellular localizations. These enzymes are a major source

of ROS in epidermal cells to maintain homeostasis (Andr, 2017) and may lead to cell injury via excessive ROS production in response to ultraviolet (UV) irradiation (Valencia and Kochevar, 2008; Glady et al., 2018). Therefore, the cells were treated with the widely used Nox inhibitor, diphenyleneiodonium chloride (DPI), prior to EP stimulation to determine whether Nox is involved in this model. The WST-8 assay data did not show significant improvement in viability when compared to the untreated group (**Figure 8A**), which negates Nox as a main source of ROS in this system. To further confirm these findings, ROS production in cells treated with DPI and untreated cells was measured using MCLA CL and the areas under the curve were compared. The data revealed no significant difference in ROS production (**Figure 8B**). Furthermore, treating the cells with the ROS scavengers, NaN_3 and MnTMPyP, did not improve viability nor did it significantly lower ROS production with DPI pre-treatment (**Figure 9 & 10**).

HaCaT keratinocytes express functional platelet-activating factor receptors (PAF-Rs) (Travers et al., 1995) and synthesize the potent inflammatory lipid mediator, PAF (Travers et al., 1996). PAF and other PAF-R agonists are produced in response to UVRs, and ultimately cause an increase in intracellular ROS levels (Travers et al., 2010). Hydrogen peroxide is widely implicated by both inducing PAF synthesis and being intracellularly produced by PAF in immune cells (Reyes-quiroz et al., 2016). Accordingly, using the PAF-R antagonist, WEB2086, in the WST-8 assay was effective in improving the cell viability with EP stimulation. These data demonstrate that PAF-R can be a potential source of intracellular ROS production, particularly intracellular hydrogen peroxide, in this system. In order to measure the intracellular concentration of this ROS, an assay kit was used. According to the red hydrogen peroxide assay data in media only, EP released approximately 5 µM extracellular hydrogen peroxide via a normal ROS

21

cascade **(Figure 11A)**. Hydrogen peroxide at this level, however, is too low to cause oxidative distress, as it requires an extracellular concentration of approximately 10 µM or higher (Sies, 2017). Furthermore, treating the cells with WEB2086, catalase, sodium azide, and DPI showed significant alleviation of H_2O_2, but this reduction was not clearly represented **(Figure 11B)**. This is due to the abundance and high turnover rate of catalase in keratinocytes (Szczepanczyk *et al.*, 2021). Therefore, experiments using a catalase inhibitor are required to adequately measure hydrogen peroxide concentration, irrespective of catalase activity. Nonetheless, this does not entirely nullify the action of ROS scavengers in lowering the hydrogen peroxide levels.

Intracellular calcium ($[Ca^{2+}]_i$) plays a critical role in the epidermis for normal physiological functions and initiates ROS production following UV radiation (Masaki *et al.*, 2009). This rise in ROS levels could be due to the effects of calcium on the cytosolic proteins responsible for Nox activation or via the promotion of the Krebs cycle for ATP synthesis in the mitochondria (Görlach *et al.*, 2015). Thus, intracellular calcium assay method was employed to determine whether a similar phenomenon occurred in this model. The data showed a dose-dependent increase in $[Ca^{2+}]_i$ levels following EP stimulation **(Figure 12A)**. Furthermore, treatment of cells with WEB2086 or DPI notably alleviated $[Ca^{2+}]_i$ levels **(Figure 12B)**. These results are consistent with those of a previous study in which a dose-dependent increase in calcium and ROS levels was noted with PAF stimulation, and the addition of DPI inhibited this production (Goldman, Moshonov and Zor, 1999).

Lastly, the skin relies heavily on the production of ATP as it is a high turnover organ and undergoes constant regeneration. This production is mainly dependent on the oxidative

phosphorylation and the electron transport chain (ETC) in the mitochondria, which leads to the release of ROS as natural bioproducts (Sreedhar, Aguilera-Aguirre and Singh, 2020). The ETC is a system composed of transmembrane protein complexes (I−IV) located in the inner membrane of the mitochondrion, and is responsible for electron leakage leading to the production of superoxide radicals and hydrogen peroxide (Zhao *et al.*, 2019). Therefore, the cells were pre-treated with ETC inhibitors: rotenone (RT), antimycin A (AA), and thenoyltrifluoroacetone (TTFA), to investigate if the mitochondria are important contributors to the secondary ROS following EP simulation. According to the WST-8 assay data, pre-treatment with RT and AA did not significantly improve viability with singlet oxygen stimulation when compared to the EP only group (**Figure 13**). However, confocal microscopy with Si-DMA fluorescence probe revealed consequent intramitochondrial singlet oxygen with EP exposure for 30 minutes (**Figure 14**), which was alleviated with ETC inhibitors treatment (**Figure 15A**). This is consistent with the theory that singlet oxygen is the main ROS produced during oxidative phosphorylation in normal cells' mitochondria (Wojtovich and Foster, 2014), and that its generation in the respiratory chain is a necessary step in ATP production (Veiga Moreira, Schwartz and Jolicoeur, 2020). Interestingly, treating the cells with the ROS scavengers targeting singlet oxygen and intracellular superoxide, and WEB2086 effectively reduced intramitochondrial singlet oxygen production (**Figure 15B & 16**); which is consistent with hydrogen peroxide assay, WST-8 assay, and CL data. Similarly, pre-treatment with DPI failed to suppress this production (**Figure 15C**), further disputing Nox as a source.

In conclusion, this study highlights the possibility of an indirect sustained release of intracellular ROS in response to singlet oxygen obtained via thermal decomposition of EP. These ROS are potentially generated through PAF-Rs and mitochondria via a calcium sensitive pathway. Alternatively, WST-8 and CL data disputed Nox involvement in this model with respect to ROS production. However, intracellular calcium and hydrogen peroxide assays revealed a minimal participation of this family of enzymes. **Figure 18** illustrates the findings and hypothesised pathways of this study. Further investigations are required to better understand the roles of Nox and PAF in this system, and to identify which secondary ROS is responsible for this phenomenon.

5. References

1) Agnez-lima, L. F. et al. (2012) 'DNA damage by singlet oxygen and cellular protective mechanisms', Mutation Research/Reviews in Mutation Research, 751, pp. 15–28. doi: 10.1016/j.mrrev.2011.12.005.

2) Andr, D. (2017) 'Reactive Oxygen Species and NOX Enzymes Are Emerging as Key Players in Cutaneous Wound Repair', International Journal of Molecular Sciences, 18(2149). doi: 10.3390/ijms18102149.

3) Benedyk, M. et al. (2007) 'HaCaT Keratinocytes Overexpressing the S100 Proteins S100A8 and S100A9 Show Increased NADPH Oxidase and NF- kB Activities', The Society for Investigative Dermatology, 21, pp. 2001–2011. doi: 10.1038/sj.jid.5700820.

4) Bickers, D. R. and Athar, M. (2006) 'Oxidative Stress in the Pathogenesis of Skin Disease', Journal of Investigative Dermatology, 126(12), pp. 2565–2575. doi: 10.1038/sj.jid.5700340.

5) Chamulitrat, W. et al. (2004) 'A Constitutive NADPH Oxidase-Like System Containing gp91 phox Homologs in Human Keratinocytes', Journal of Investigative Dermatology, 122(4), pp. 1000–1009. doi: 10.1111/j.0022-202X.2004.22410. x.

6) Devasagayam, T. P. A. and Kamat, J. P. (2002) 'Biological significance of singlet oxygen', Indian Journal of Experimental Biology, 40, pp. 680–692.

7) Glady, A. et al. (2018) 'Involvement of NADPH oxidase 1 in UVB-induced cell signalling and cytotoxicity in human keratinocytes', Biochemistry and Biophysics Reports, 14, pp. 7–15. doi: 10.1016/j.bbrep.2018.03.004.

8) Goldman, R., Moshonov, S. and Zor, U. (1999) 'Calcium-dependent PAF-stimulated generation of reactive oxygen species in a human keratinocyte cell line', Biochimica et Biophysica Acta - Molecular and Cell Biology of Lipids, 1438(3), pp. 349–358. doi: 10.1016/S1388-1981(99)00066-9.

9) Görlach, A. et al. (2015) 'Calcium and ROS: A mutual interplay', Redox Biology, 6, pp. 260–271. doi: 10.1016/j.redox.2015.08.010.

10) Hrycay, E. G. and Bandiera, S. M. (2015) 'Involvement of Cytochrome P450 in Reactive Oxygen Species Formation and Cancer', in Advances in Pharmacology. 1st edn. Vancouver, Canada, Elsevier Inc., p. 14. doi: 10.1016/bs.apha.2015.03.003.

11) Kim, J. S. et al. (2019) 'A quantitative method to measure low levels of ros in nonphagocytic cells by using a chemiluminescent imaging system', Oxidative Medicine and Cellular Longevity, 2019. doi: 10.1155/2019/1754593.

12) Masaki, H. et al. (2009) 'Reactive Oxygen Species in HaCaT Keratinocytes After UVB Irradiation Are Triggered by Intracellular Ca2+ Levels', Journal of Investigative Dermatology, 14(1), pp. 50–52. doi: 10.1038/jidsymp.2009.12.

13) Nagaoka, Y. et al. (2005) 'Specific inactivation of cysteine protease-type cathepsin by singlet oxygen generated from naphthalene endoperoxides', Biochemical and Biophysical Research Communications, 331, pp. 215–223. doi: 10.1016/j.bbrc.2005.03.146.

14) Ogilby, P. R. (2010) 'Singlet oxygen: there is indeed something new under the sun', Chemical Society Reviews, 39, pp. 3181–3209. doi: 10.1039/b926014p.

15) Otsu, K. et al. (2005) 'An abortive apoptotic pathway induced by singlet oxygen is due to the suppression of caspase activation', Biochemical journal, 389, pp. 197–206. doi: 10.1042/BJ20042067.

16) Ouchi, A. et al. (2010) 'Kinetic study of the quenching reaction of singlet oxygen by carotenoids and food extracts in solution. development of a singlet oxygen absorption capacity (SOAC) assay method', Journal of Agricultural and Food Chemistry, 58(18), pp. 9967–9978. doi: 10.1021/jf101947a.

17) Ouedraogo, G. D. and Redmond, R. W. (2003) 'Secondary Reactive Oxygen Species Extend the Range of Photosensitization Effects in Cells: DNA Damage Produced Via Initial Membrane Photosensitization', Photochemistry and Photobiology, 77(2), pp. 192–203.

18) Pierlo, C. et al. (2000) 'Naphthalene Endoperoxides as Generators of Singlet Oxygen in Biological Media', Methods in Enzymology, 319 (1997), pp. 3–20.

19) Ray, P. D., Huang, B.-W. and Tsuji, Y. (2012) 'Reactive oxygen species (ROS) homeostasis and redox regulation in cellular signalling', Cellular signalling, 24(5), pp. 981–990. doi: 10.1016/j.cellsig.2012.01.008.

20) Reyes-quiroz, M. E. et al. (2016) 'Platelet-activating factor and hydrogen peroxide exert a dual modulatory effect on the transcription of LXR α and its target genes in human neutrophils', International Immunopharmacology, 38, pp. 357–366. doi: 10.1016/j.intimp.2016.05.001.

21) Sies, H. (2017) 'Hydrogen peroxide as a central redox signaling molecule in physiological oxidative stress: Oxidative eustress', Redox Biology, 11, pp. 613–619. doi: 10.1016/j.redox.2016.12.035.

22) Sreedhar, A., Aguilera-Aguirre, L. and Singh, K. K. (2020) 'Mitochondria in skin health, aging, and disease', Cell Death and Disease, 11(6). doi: 10.1038/s41419-020-2649-z.

23) Szczepanczyk, M. et al. (2021) 'Catalase Activity in Keratinocytes, Stratum Corneum, and Defatted Algae Biomass as a Potential Skin Care Ingredient', Biomedicines, 9(12), pp. 1–19.

24) Travers, J. B. et al. (1995) 'Identification of Functional Platelet-Activating Factor Receptors on Human Keratinocytes', Journal of Investigative Dermatology, 105(6), pp. 816–823. doi: 10.1111/1523-1747.ep12326581.

25) Travers, J. B. et al. (1996) 'Platelet-Activating Factor Biosynthesis Induced by Various Stimuli in Human HaCaT Keratinocytes', Journal of Investigative Dermatology, 107(1), pp. 88–94. doi: 10.1111/1523-1747.ep12298295.

26) Travers, Jared B et al. (2010) 'Ultraviolet B Radiation of Human Skin Generates Platelet activating Factor Receptor Agonists', Photochemistry and photobiology, 86(4), pp. 949–954. doi: 10.1111/j.1751-1097.2010.00743. x.

27) Valencia, A. and Kochevar, I. E. (2008) 'Nox1-based NADPH oxidase is the major source of UVA-induced reactive oxygen species in human keratinocytes', Journal of Investigative Dermatology, 128(1), pp. 214–222. doi: 10.1038/sj.jid.5700960.

28) Veiga Moreira, J. da, Schwartz, L. and Jolicoeur, M. (2020) 'Targeting Mitochondrial Singlet Oxygen Dynamics Offers New Perspectives for Effective Metabolic Therapies of Cancer', Frontiers in Oncology, 10, pp. 1–15. doi: 10.3389/fonc.2020.573399.

29) Wojtovich, A. P. and Foster, T. H. (2014) 'Optogenetic control of ROS production', Redox Biology, 2(1), pp. 368–376. doi: 10.1016/j.redox.2014.01.019.

30) Yamaguchi, S. et al. (2010) 'Evaluation of chemiluminescence reagents for selective detection of reactive oxygen species', Analytica Chimica Acta, 665(1), pp. 74–78. doi: 10.1016/j.aca.2010.03.025.

31) Zhao, R. U. Z. et al. (2019) 'Mitochondrial electron transport chain, ROS generation and uncoupling (Review)', International Journal of Molecular Medicine, 44, pp. 3–15. doi: 10.3892/ijmm.2019.4188.

6. Figures
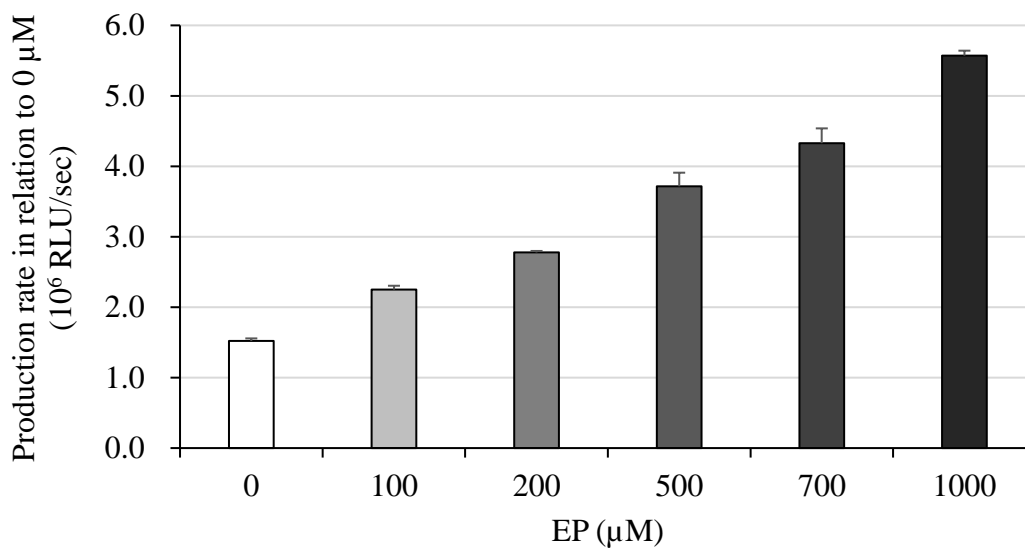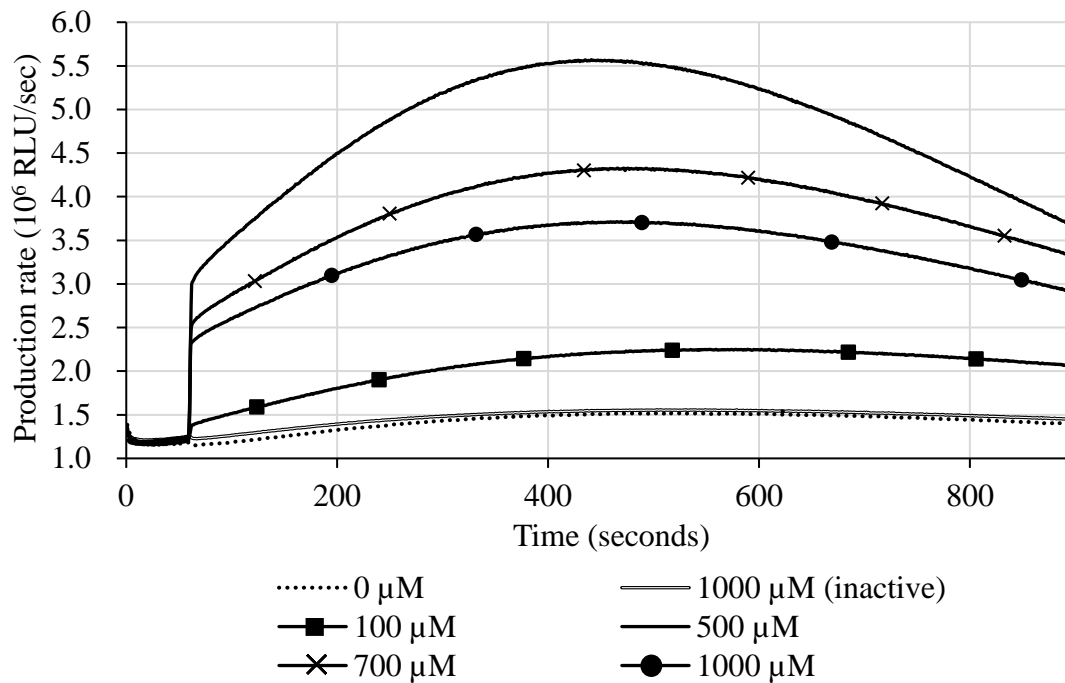
Figure 1 MCLA CL curve and peak-base graph of singlet oxygen production rate from EP solutions of varying concentrations. Values are reported as means $\pm$ S.D. ($n = 3$–6).
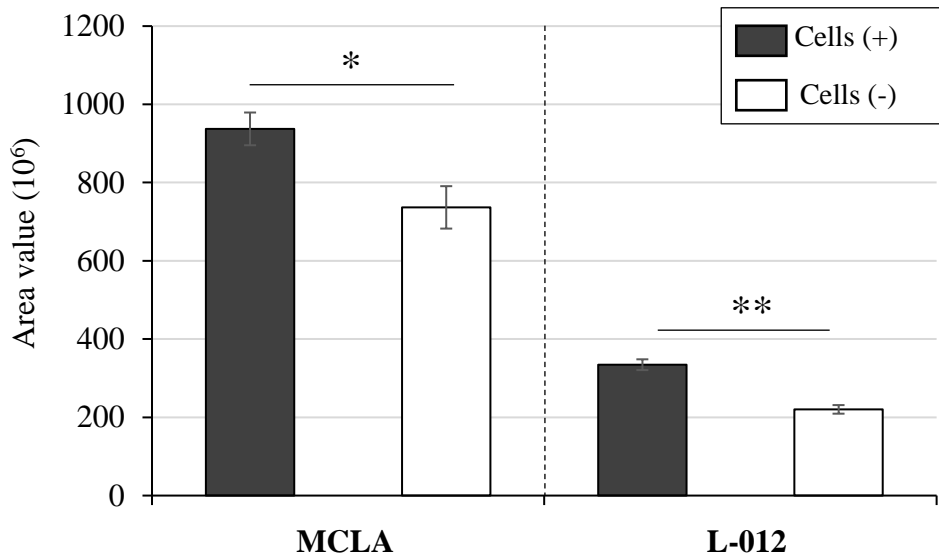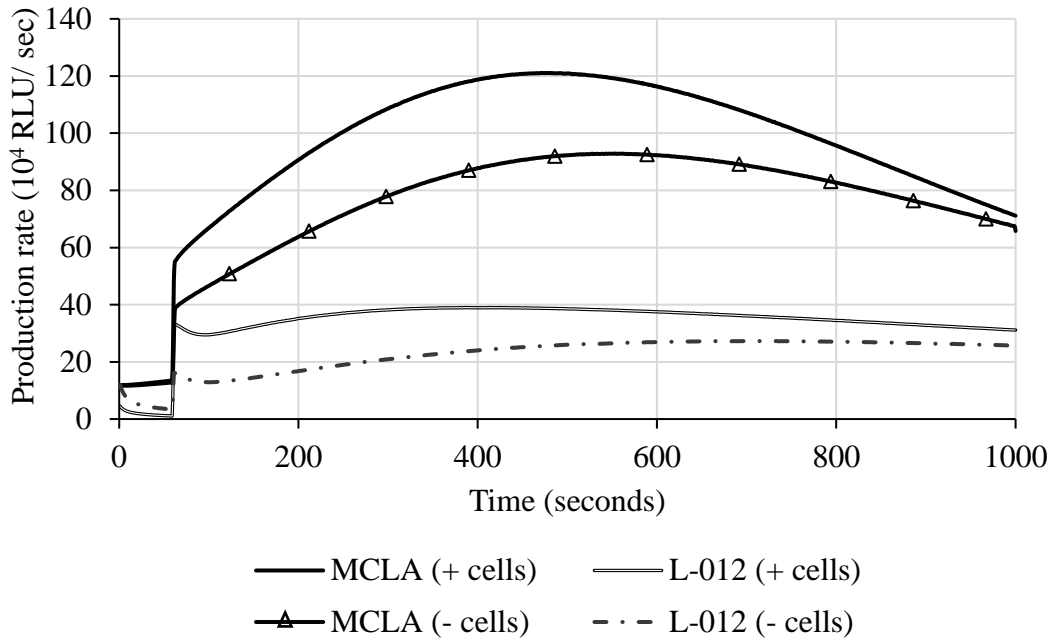
Figure 2 CL curves and area under the curve (AUC) graphs for ROS production rate with 1 mM EP solution using MCLA and L-012 reagents. Sample solutions containing HaCaT keratinocytes were also measured with each reagent. Values are reported as means $\pm$ S.D. ($n = 5$–8); * $p < 0.05$, ** $p < 0.01$.

.

A.
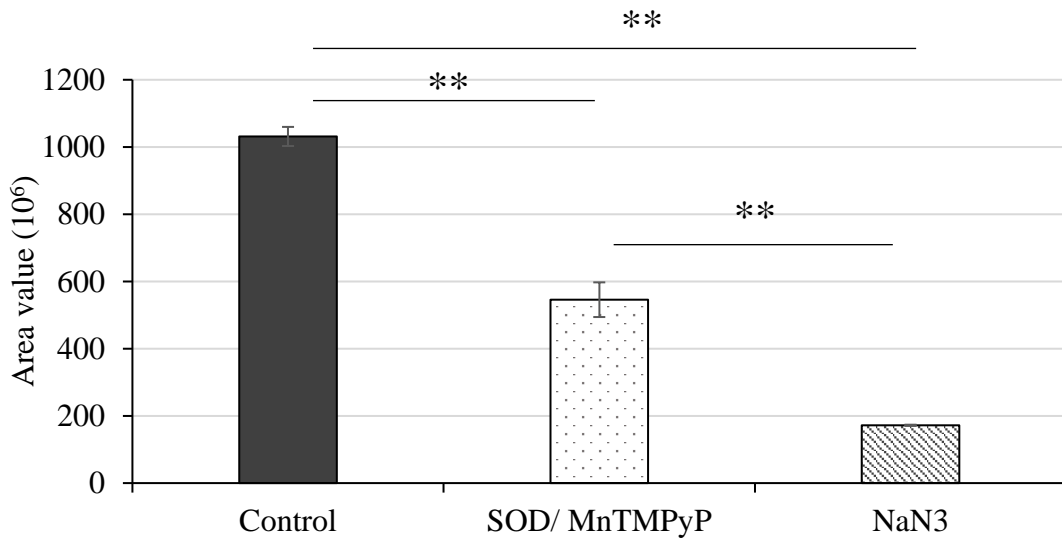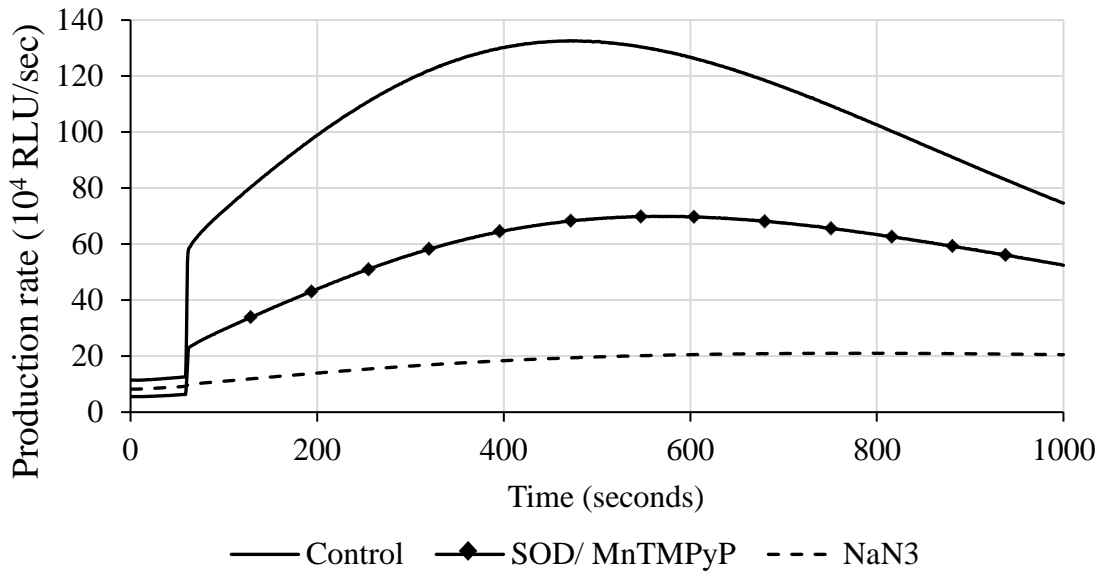
B.
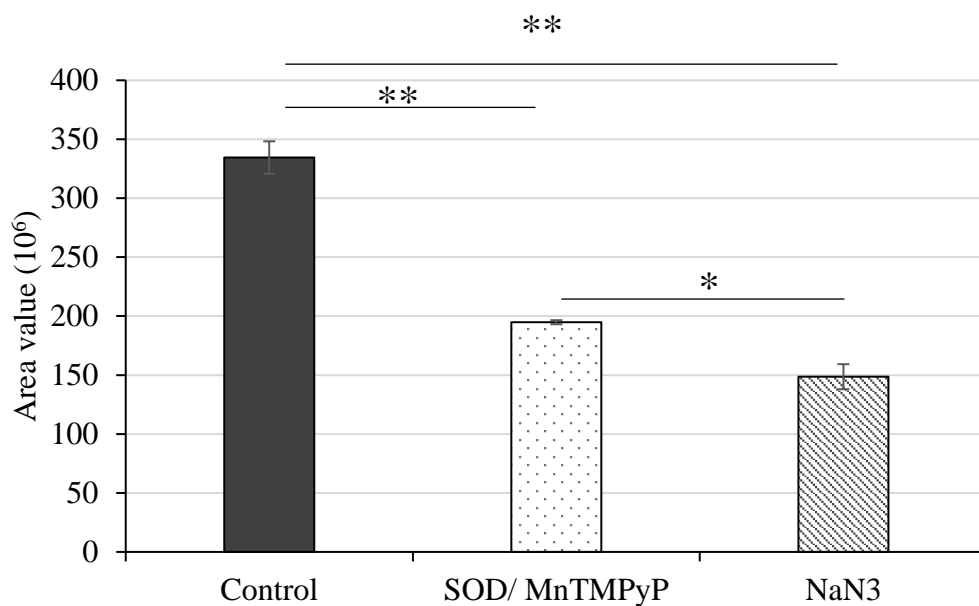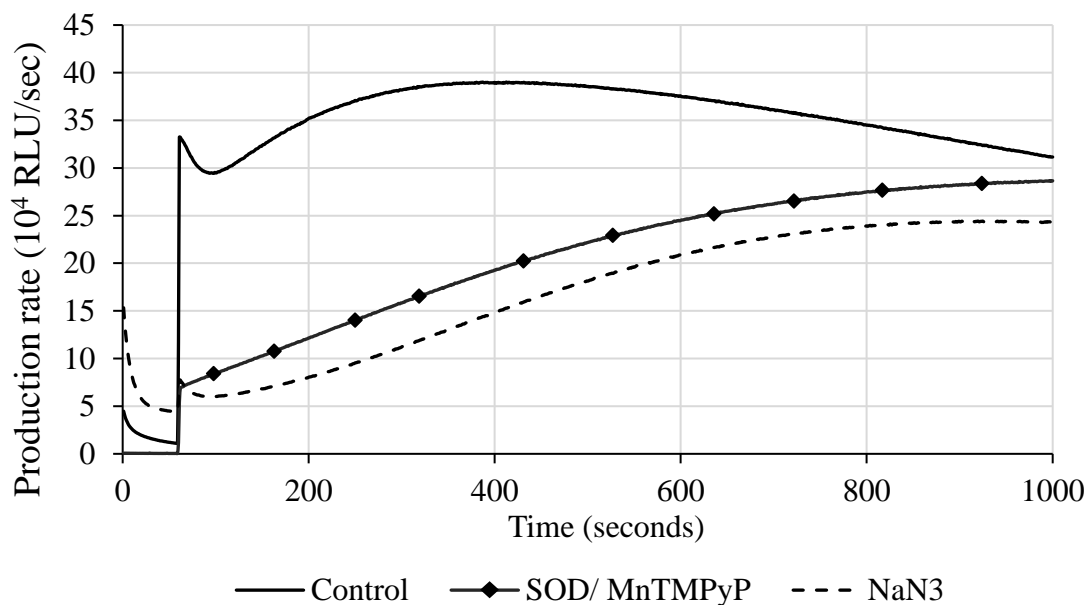
Figure 3 CL curves and AUC graphs for ROS production with 1 mM EP. (A) MCLA, **(B)** L-012 in the presence of HaCaT keratinocytes and ROS scavengers. Values are reported as means ± S.D. ($n = 3–4$); * $p < 0.05$, ** $p < 0.01$.
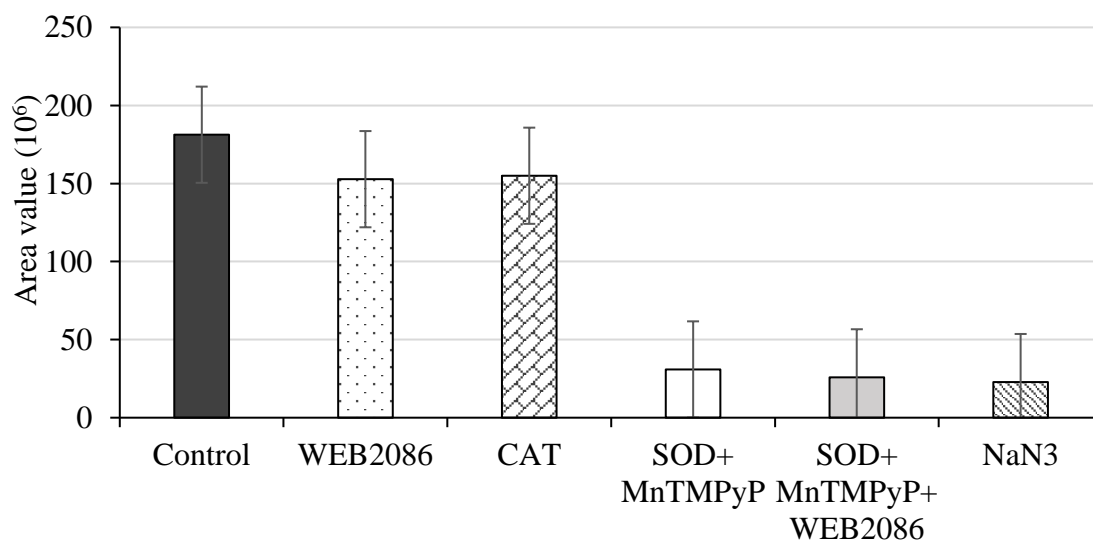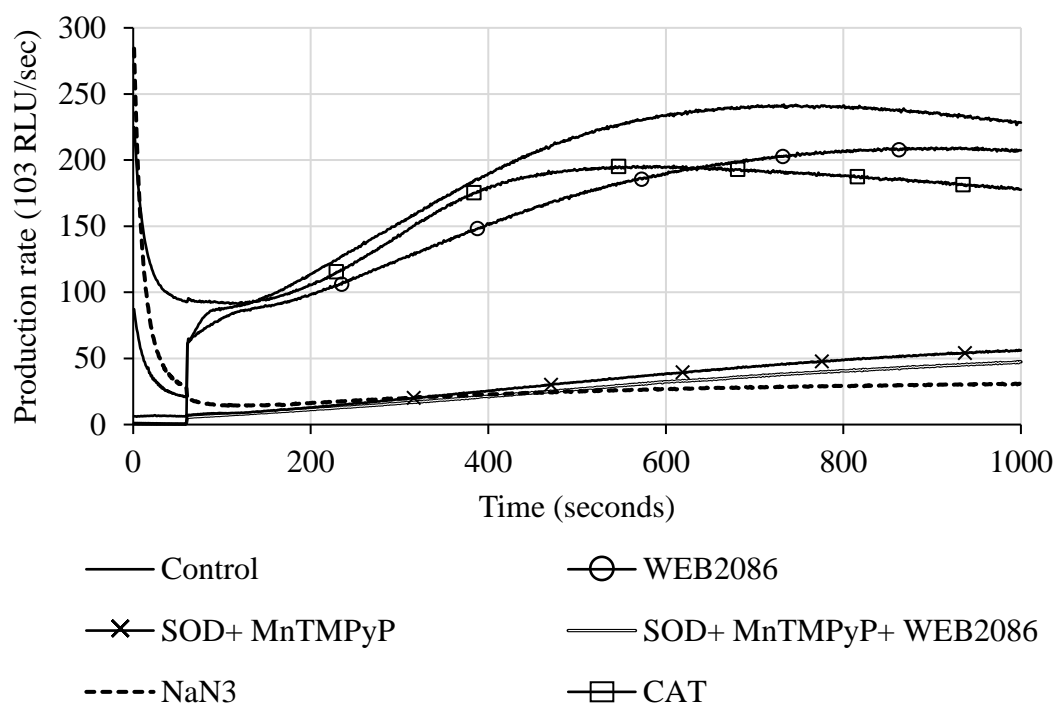
Figure 4 L-012 CL curve and AUC graph for ROS production with 1 mM EP for 1000 seconds in the presence of HaCaT keratinocytes. SOD, CAT, MnTMPyP, WEB2086, and NaN$_3$ were used at concentrations of 1,000 U/ mL, 10 μM, 10 mM, and respectively. Values are reported as means ± S.D.
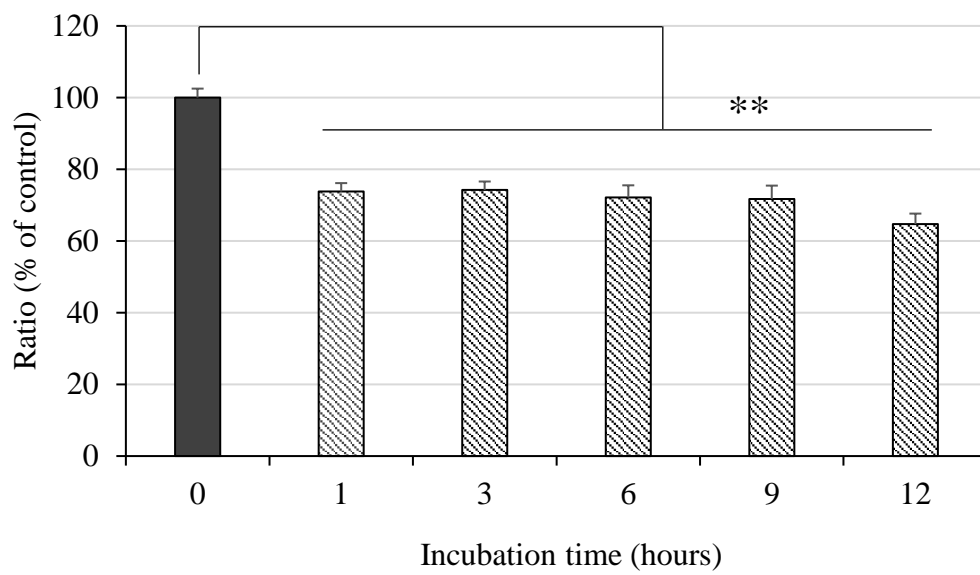
Figure 5 Cell viability assay data using WST-8 kit. The cells were incubated with 1 mM EP for 1 – 12 hours prior to reading. Values are reported as means ± S.D. ($n = 4$); ** $p <$ 0.01.

A.

Pre-incubation

B.

Co-incubation

C.
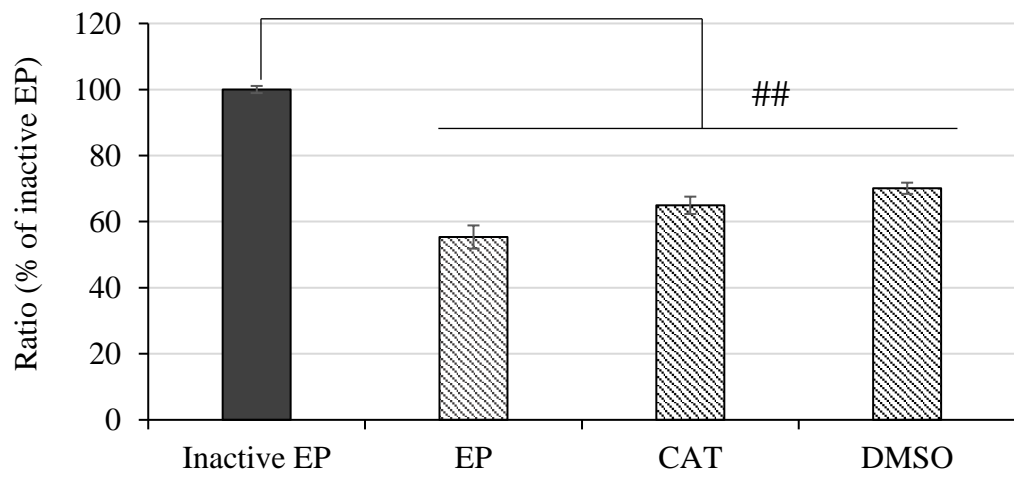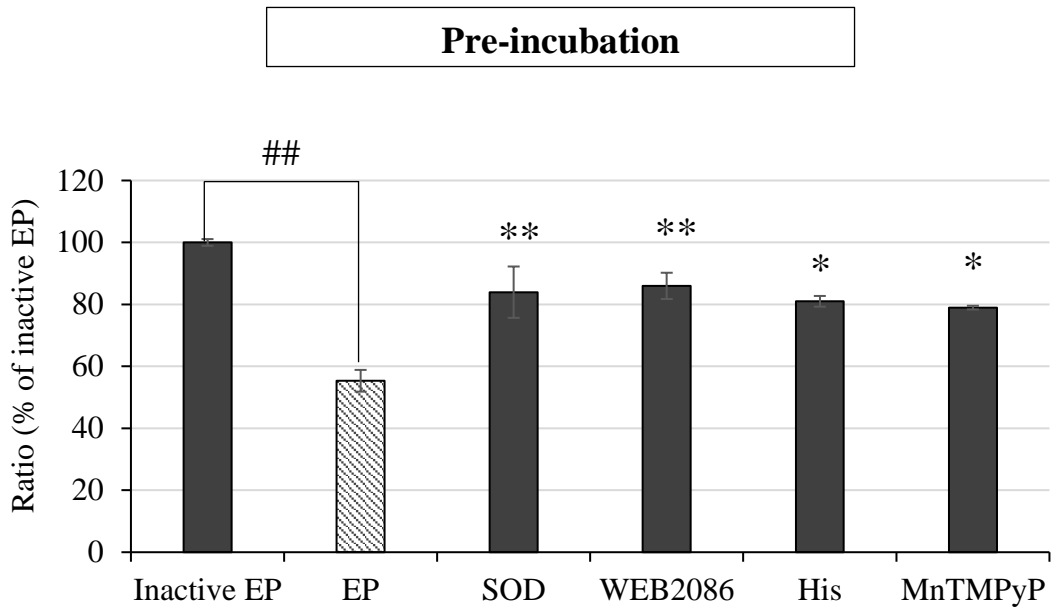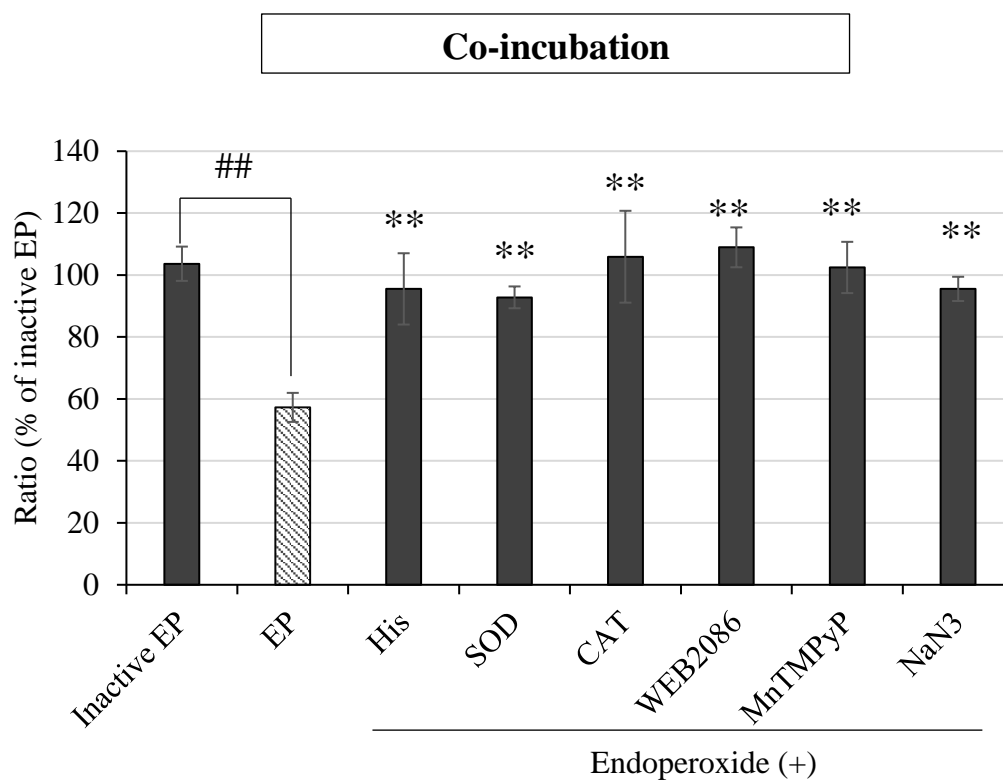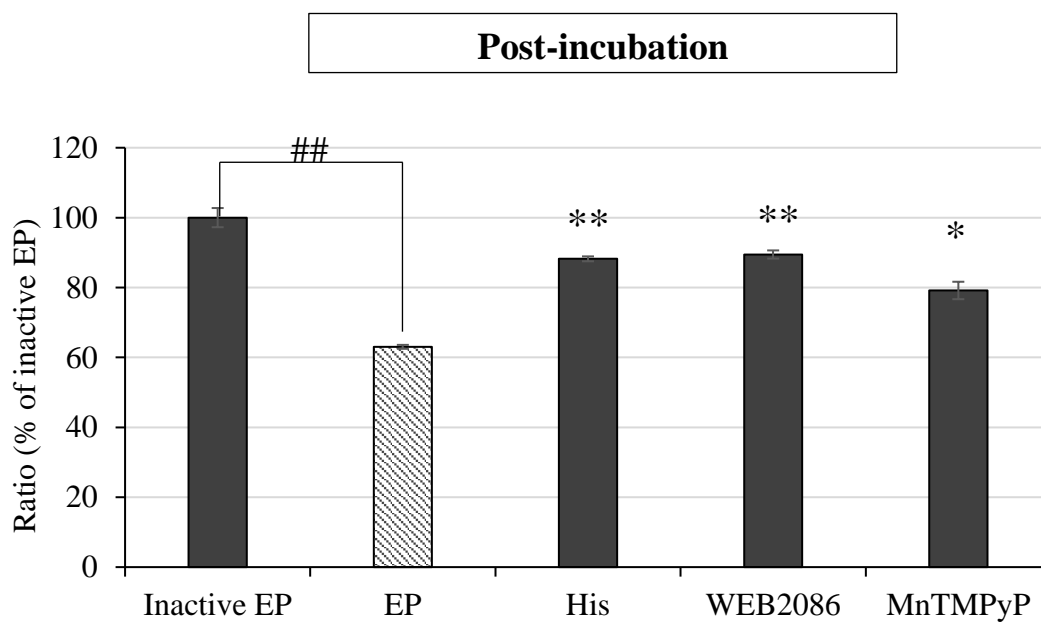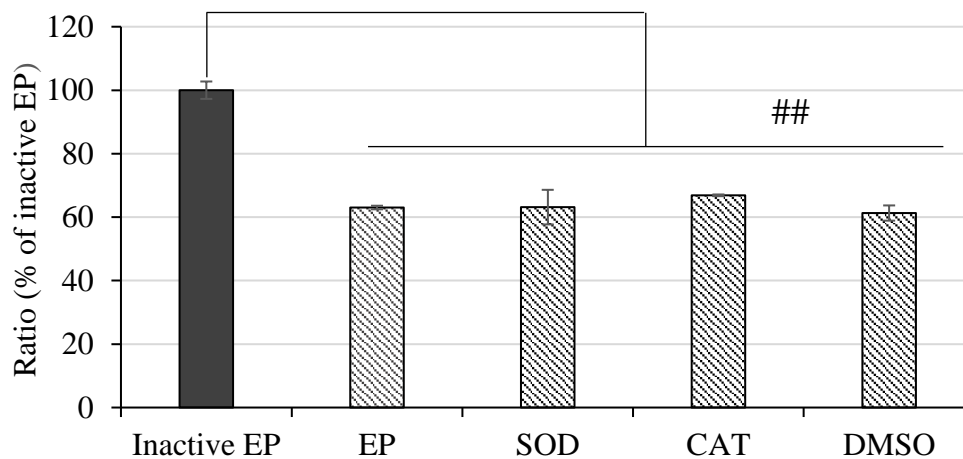
Post-incubation

Figure 6 Cell viability assay data using WST-8 kit. (A) HaCaT keratinocytes were pre-treated with the ROS scavengers for one hour, followed by 1 mM EP incubation for another hour. **(B)** In co-incubation tests, ROS scavengers were added for 10 minutes followed by the addition of 1 mM EP solution; the cells were then incubated with both for one hour. **(C)** In post-incubation tests, the cells were stimulated with 1 mM EP for one hour prior to ROS scavenger treatment for another hour. SOD: superoxide dismutase; CAT: catalase; His: histidine; NaN$_3$: sodium azide. Values are reported as means ± S.D. ($n = 3$–14); * $p < 0.05$, ** $p < 0.01$ vs EP.
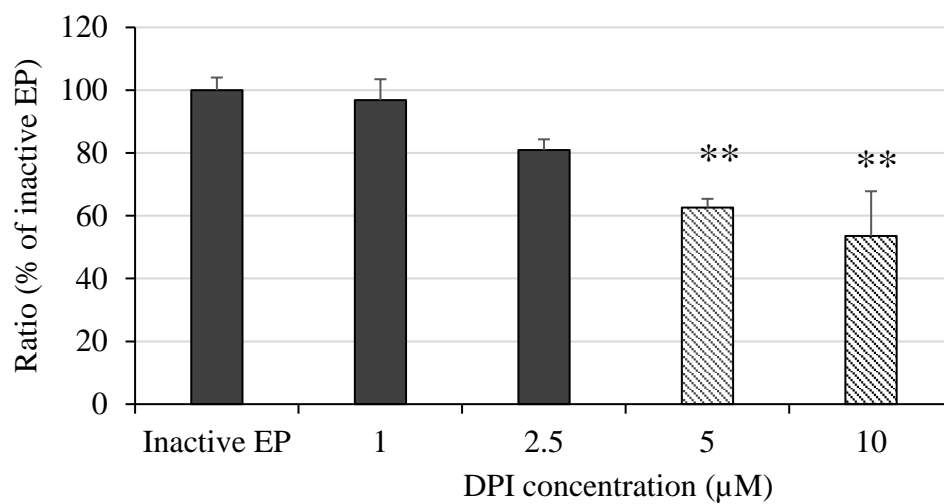
Figure 7 Cell viability assay using WST-8 kit to determine safe concentration of diphenyleneiodonium chloride (DPI) on HaCaT keratinocytes. Values are reported as means ± S.D. ($n = 5$); ** $p < 0.01$ vs inactive EP.

A.

B.

40
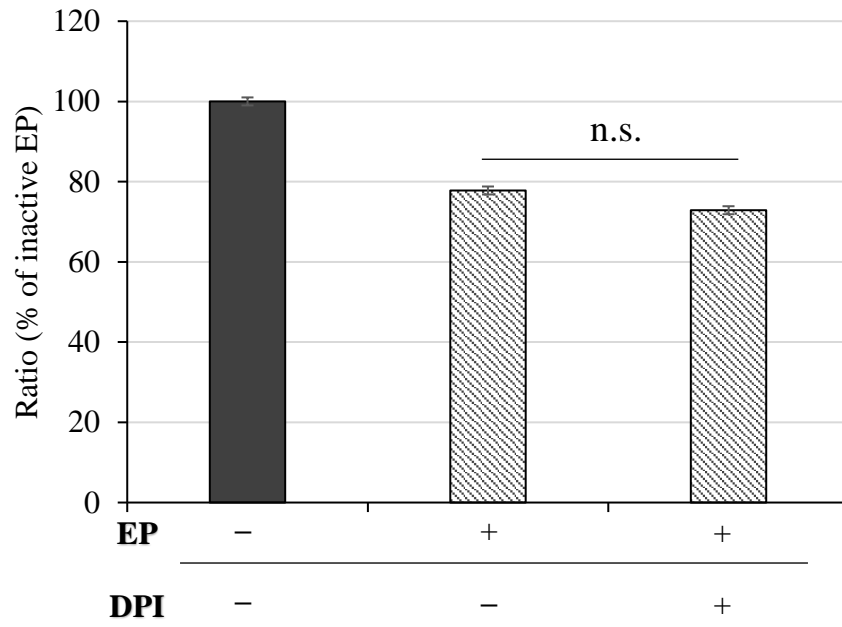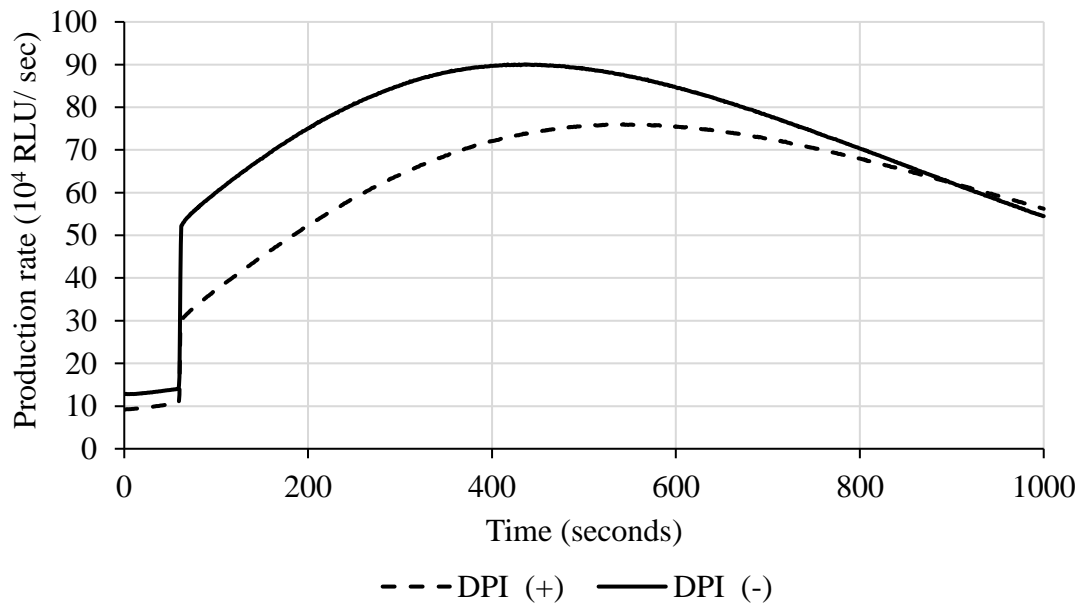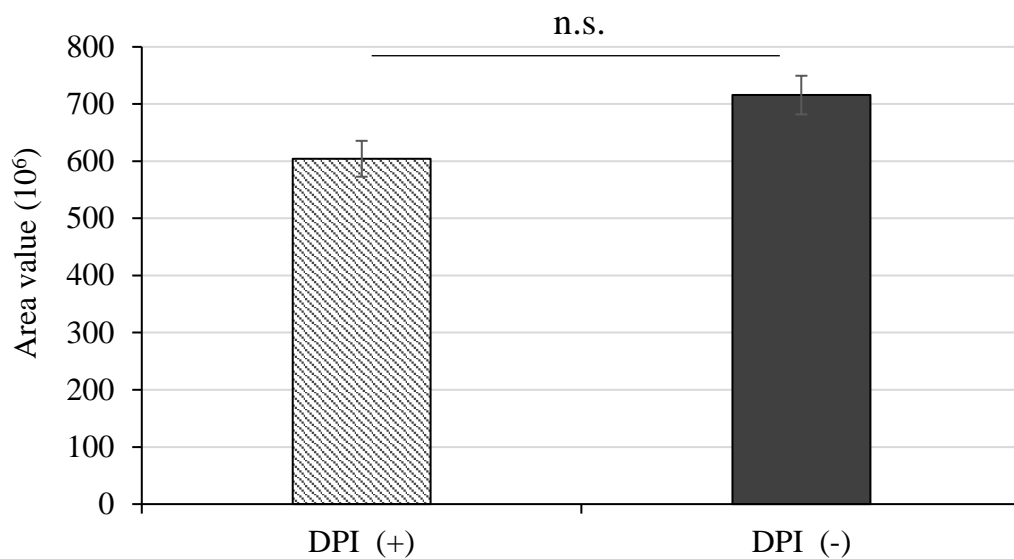
Figure 8 Involvement of Nox in this model. (A) Cell viability assay data using WST-8 kit. In the DPI treated group, cells were incubated with 2.5 µM DPI for 2 minutes prior to 1 mM EP exposure. ($n = 14$). (B) MCLA chemiluminescence curve and AUC graph for ROS production following 1 mM EP stimulation from cells. The same concentration and incubation time was used for DPI pre-treatment. Values are reported as means ± S.D. ($n = 4$–6).

A.

DPI	–	+	–	+	–
EP	–	–	+	+	+
NaN₃	–	–	–	+	+
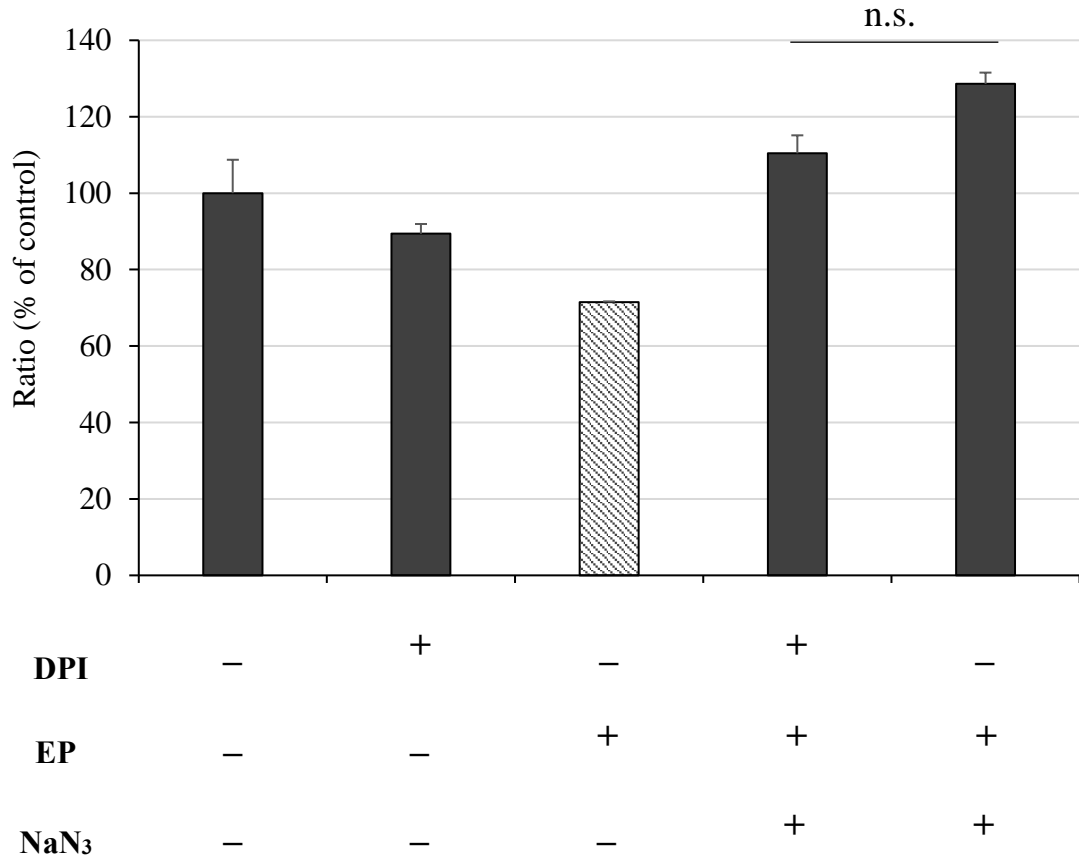
B.
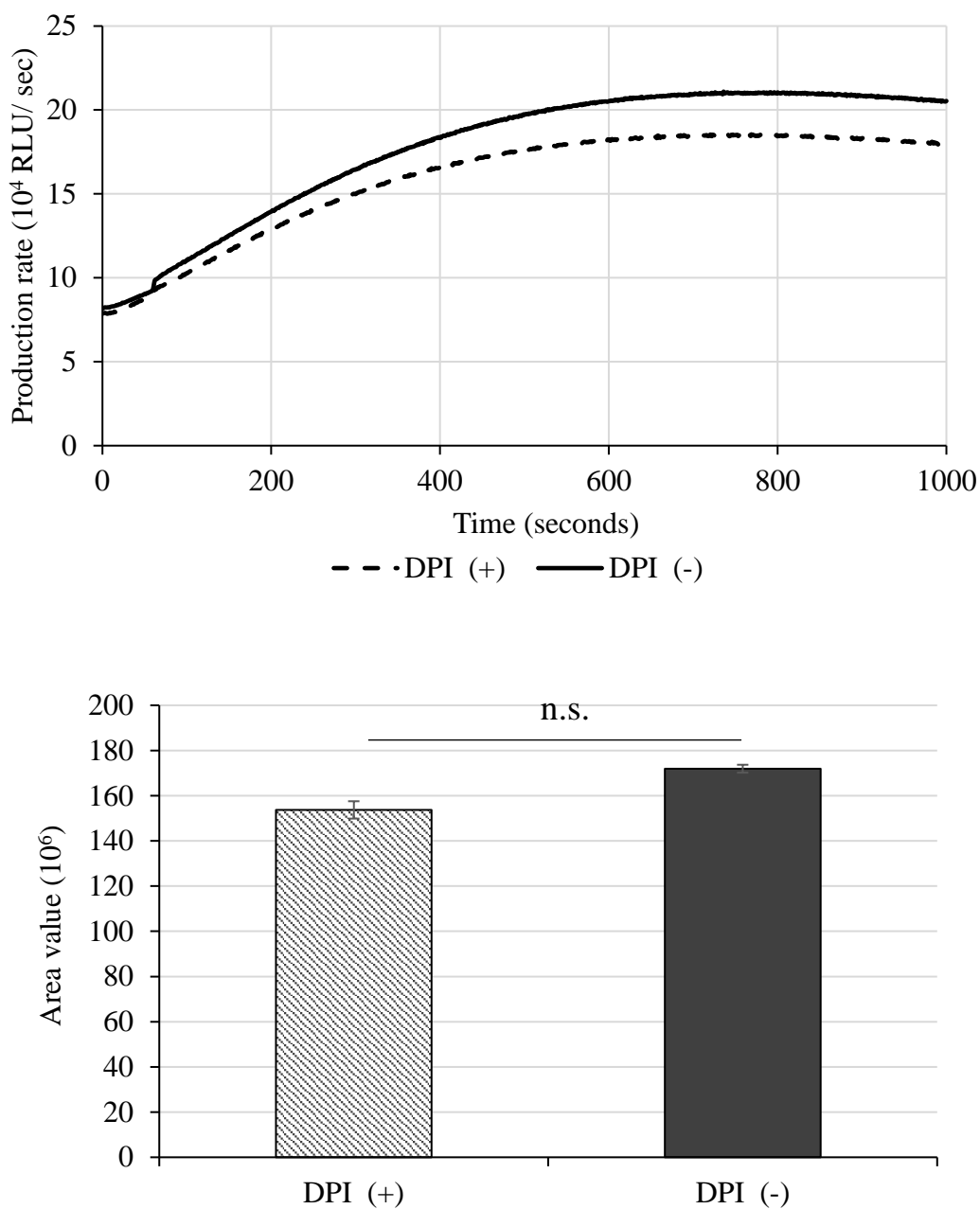
Figure 9 Involvement of Nox with ROS scavengers targeting $^1O_2$ (A) Cell viability assay data using WST-8 kit. Cells were treated with DPI for 2 minutes, then treated with 1 mM NaN3 and EP stimulation. (n = 5). (B) MCLA CL curve and AUC graph for ROS production following 1 mM NaN3 and EP stimulation from cells. The same concentration and incubation time was used for DPI pre-treatment. Values are reported as means ± S.D. (*n* = 3–4).

A.

DPI	–	+	–	+	–
EP	–	–	+	+	+
MnTMPyP	–	–	–	+	+
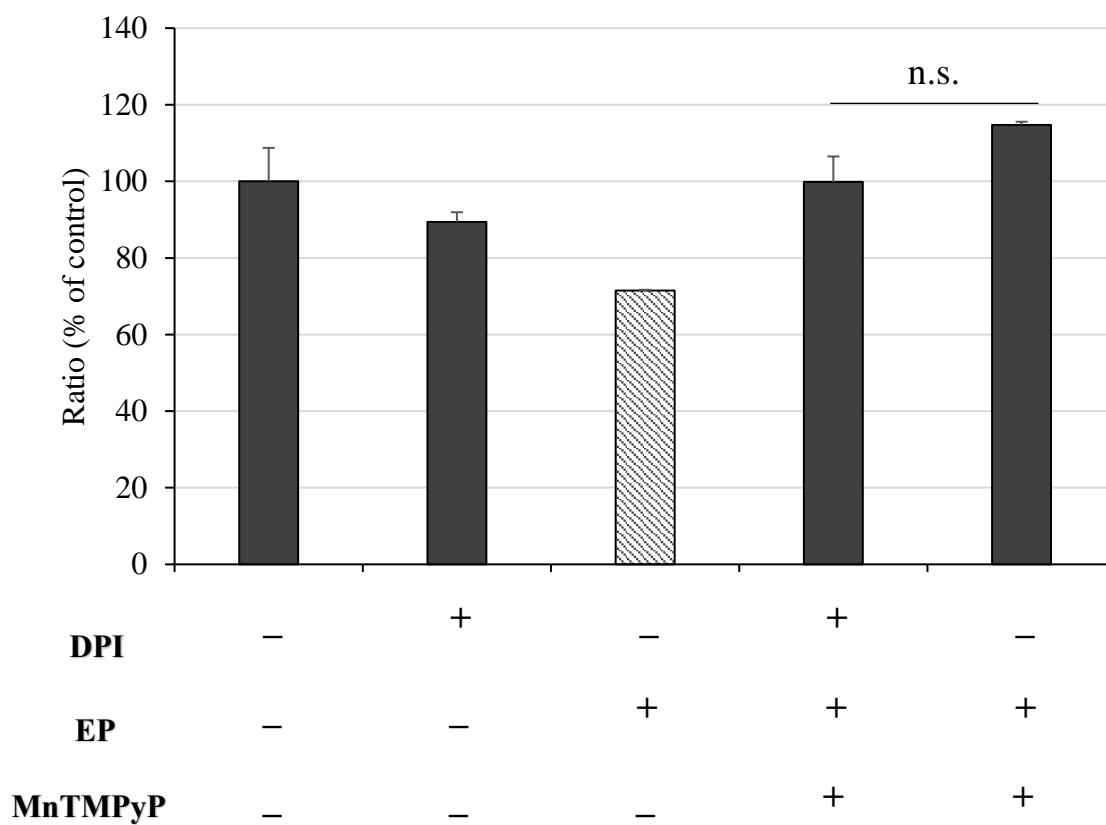
B.
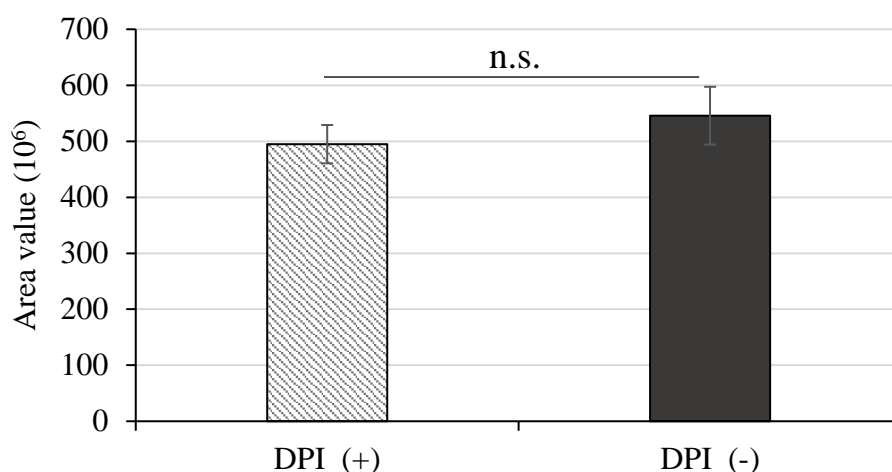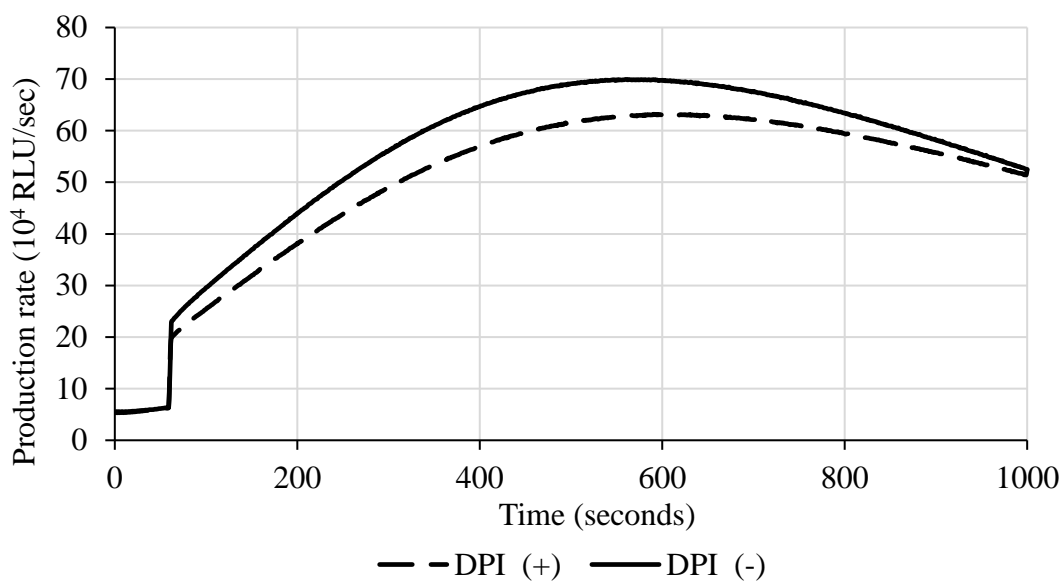
Figure 10 Involvement of Nox with ROS scavengers targeting O_2^- (A) Cell viability assay data using WST-8 kit. Cells were treated with DPI for 2 minutes, then treated with 10 µM MnTMPyP and EP stimulation. ($n = 5$). **(B)** MCLA CL curve and AUC graph for ROS production following 1000 U/ mL SOD and 10 µM MnTMPyP and EP stimulation from cells. The same concentration and incubation time was used for DPI pre-treatment. Values are reported as means ± S.D. ($n = 3$).

A.
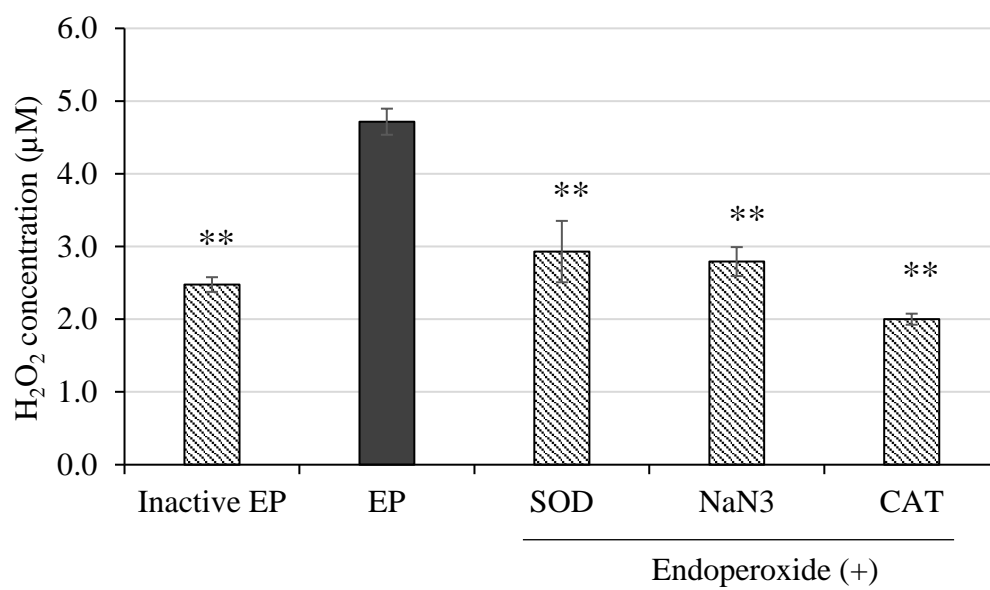
B.
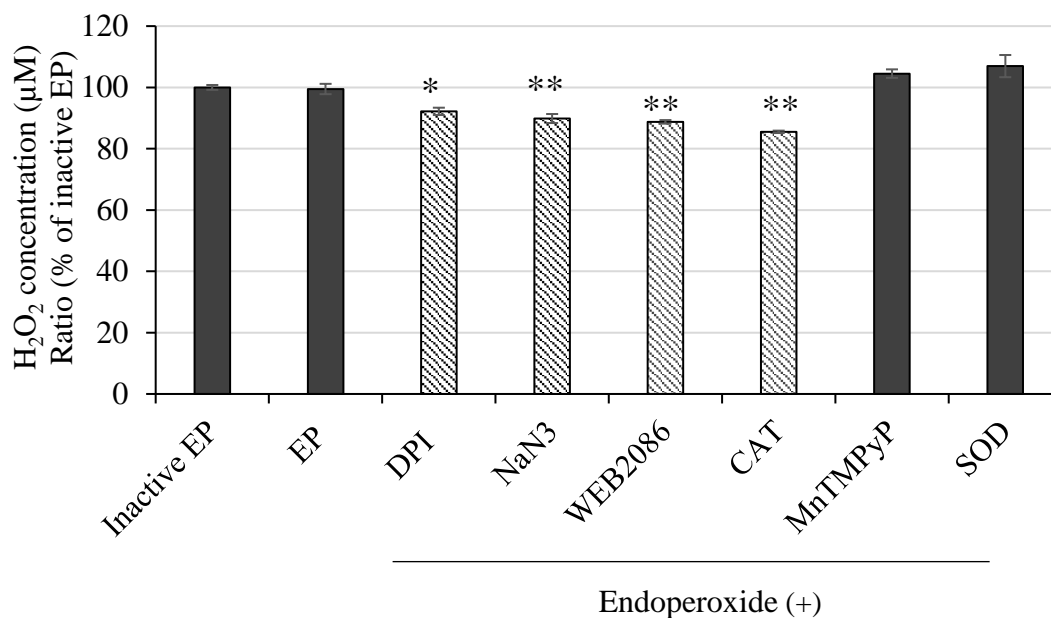
Figure 11 Quantification of hydrogen peroxide concentration using red hydrogen peroxide assay kit. (A) ROS scavengers were first added for 10 minutes to media only (i.e., no cells), followed by one-hour coincubation with 1 mM EP and fluorescence was measured. **(B)** HaCaT keratinocytes were pre-treated with ROS scavengers for 10 minutes, followed by coincubation with 1 mM EP solution for one hour (for DPI group, cells were pre-treated for 2 minutes only with 2.5 µM DPI instead). Values are reported as means ± S.D. ($n = 7–12$); * $p < 0.05$ vs EP, ** $p < 0.01$ vs EP.

A.

Figure showing a bar chart. Y-axis: Intracellular Ca^{2+} fluorescence intensity ratio (% of 0 µM EP), ranging from 0 to 160. X-axis: EP concentration (µM) with values 0, 50, 100, 500, 1000.
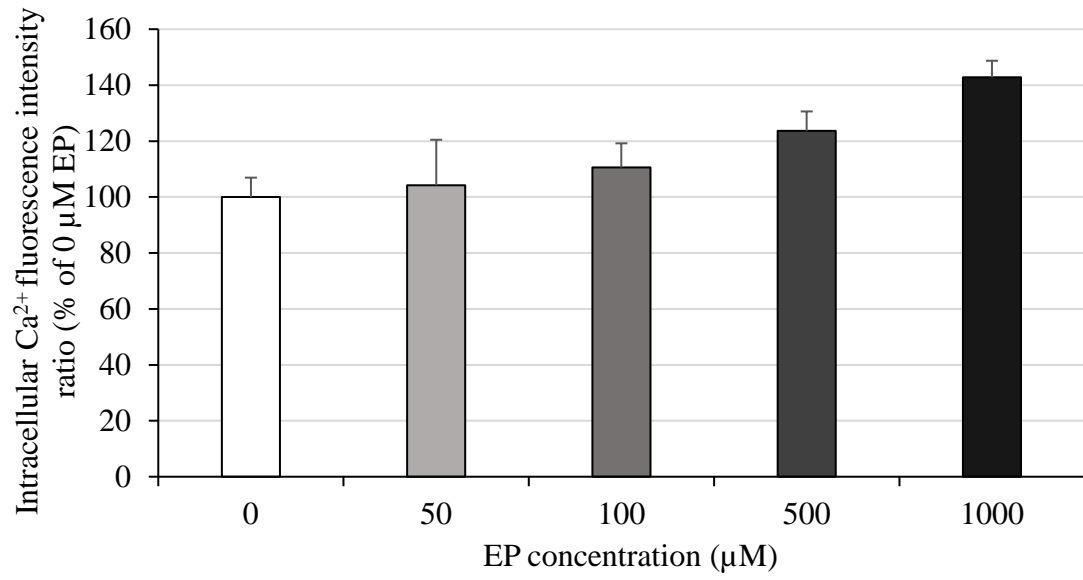
B.
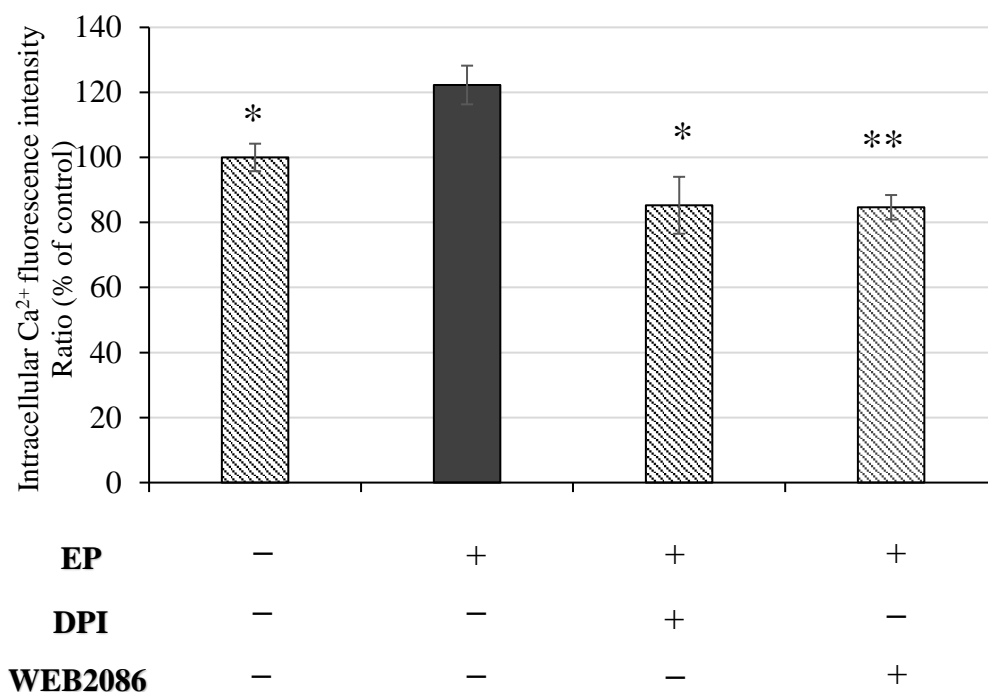
Figure 12 Quantification of intracellular calcium using Ca²⁺ II Fluo 4 kit. (A) HaCaT keratinocytes were incubated with EP solutions at concentrations of 50, 100, 500, and 1000 µM for one hour. Fluo 4AM was then added to the mixture and intracellular calcium was measured. (n = 5) (B) Cells were treated with 2.5 µM DPI or 10 µM WEB2086 prior to the one-hour incubation with EP and fluorescence reading. Values are reported as means ± S.D. (n = 21–28); * p < 0.05, ** p < 0.01 vs 1 mM EP.

A.
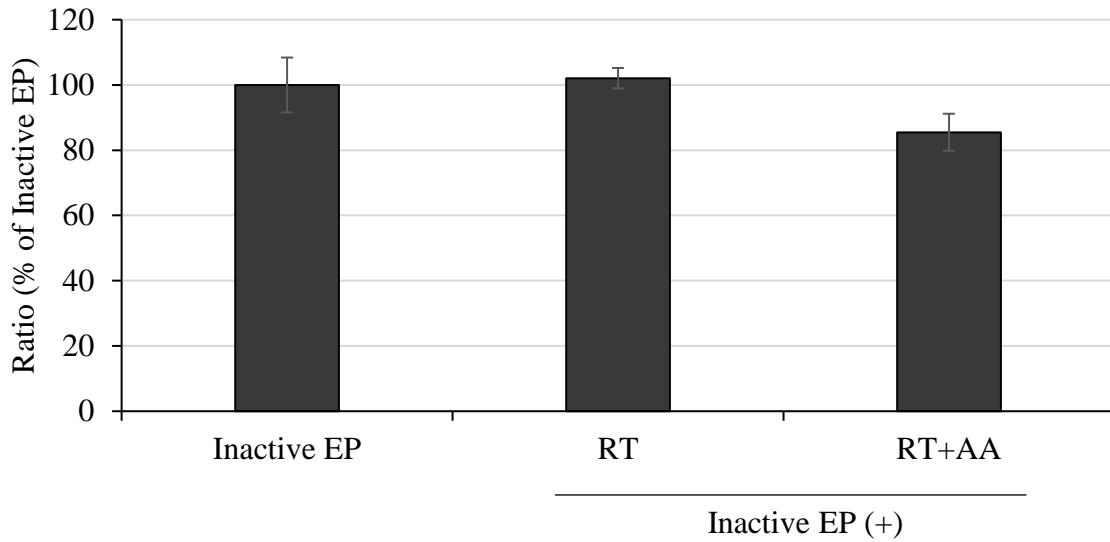
B.
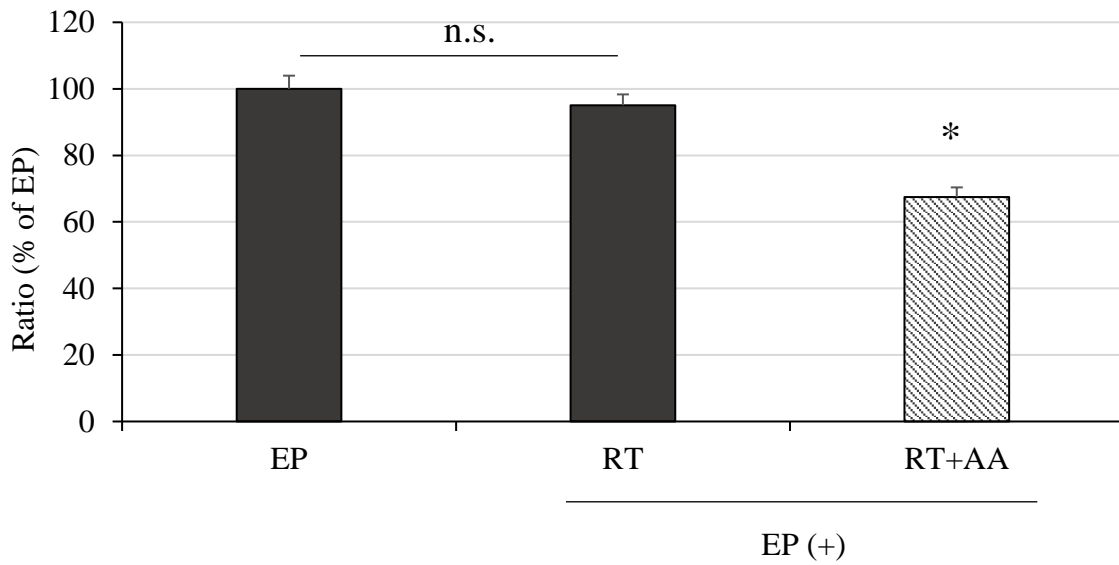
Figure 13 Cell viability assay with electron transport chain (ETC) inhibitors. Cells were treated for 2 minutes with rotenone (RT) and antimycin A (AA) at concentrations of 5 µM and 25 µM respectively prior to EP stimulation. Values are reported as means ± S.D. ($n = 4$); * $p < 0.05$ vs EP.

	Merged	**Mito-Bright**	**$^1O_2$**
Inactive EP			
EP (-)			
EP (+)			
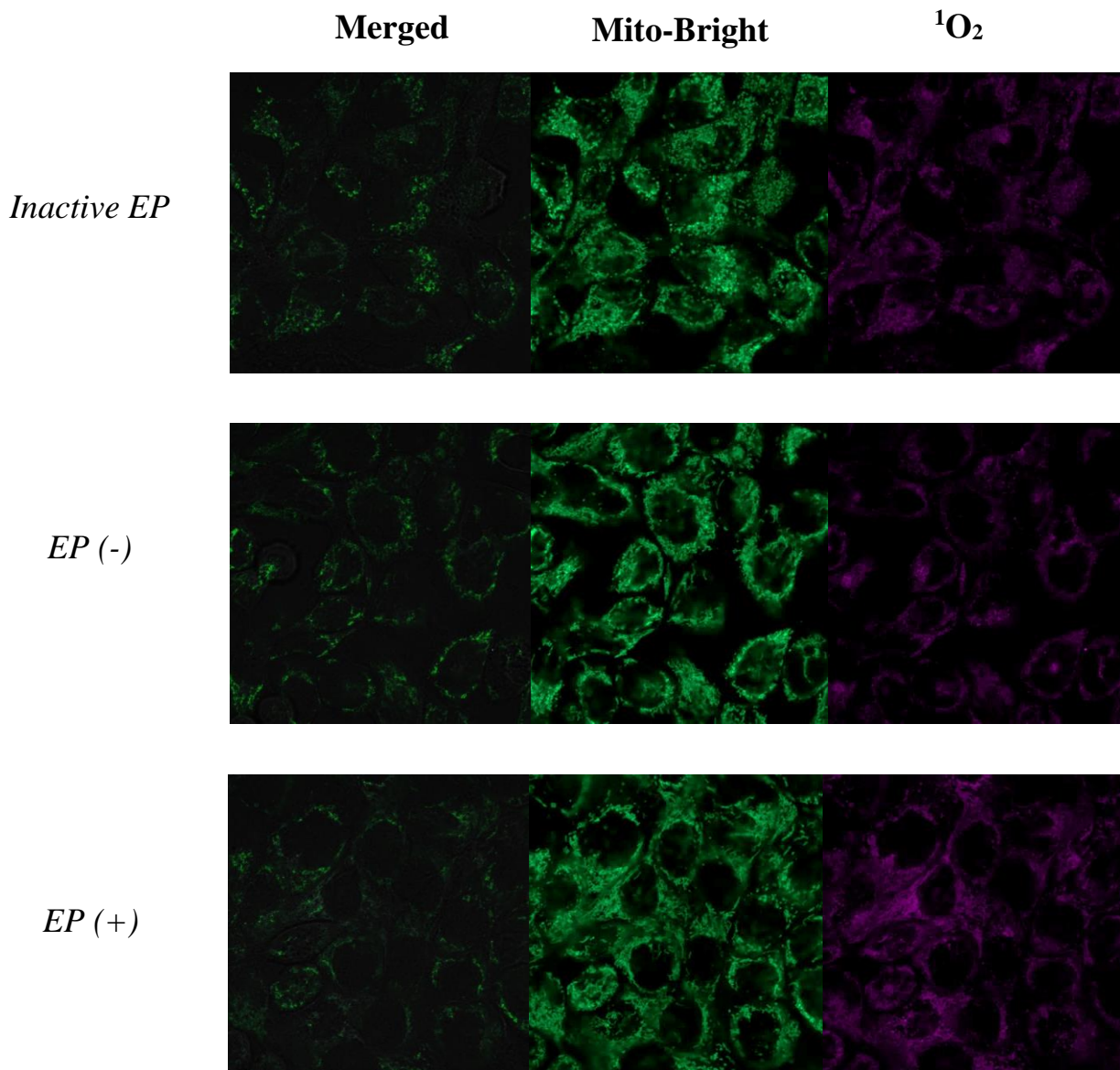
Figure 14 Si-DMA for mitochondrial $^1O_2$ imaging following 1 mM EP stimulation for 30 minutes.

A.
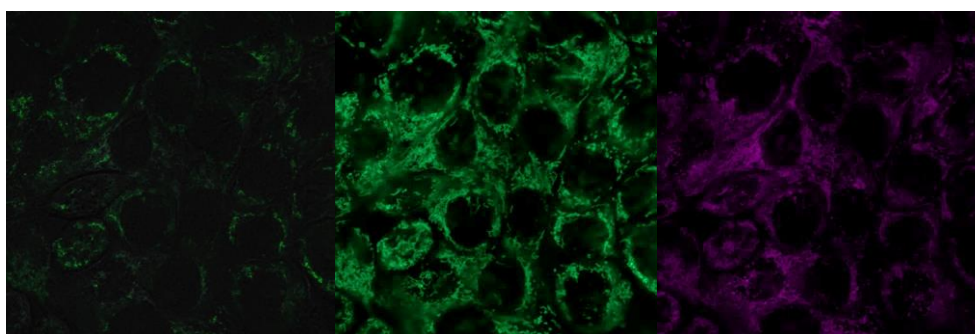
	Merged	Mito-Bright	$^1O_2$
EP (+)			
EP + RT+AA+TT			
Inactive EP + RT+AA+TT			
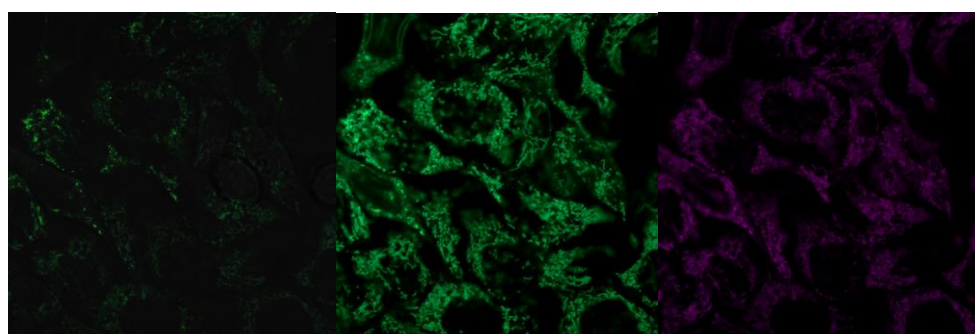
B.
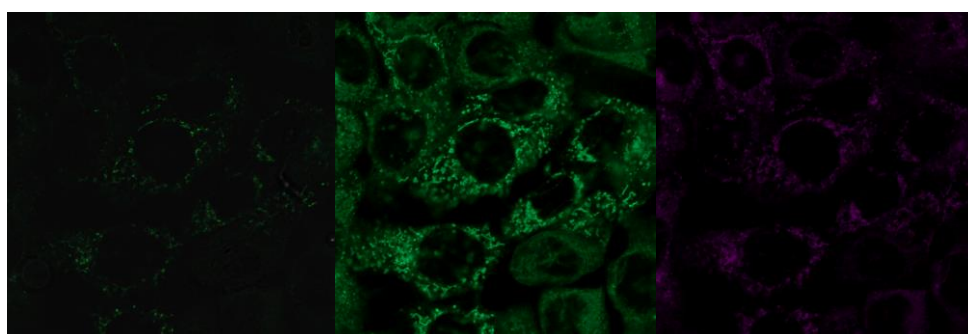
	Merged	Mito-Bright	$^1O_2$

EP (+)
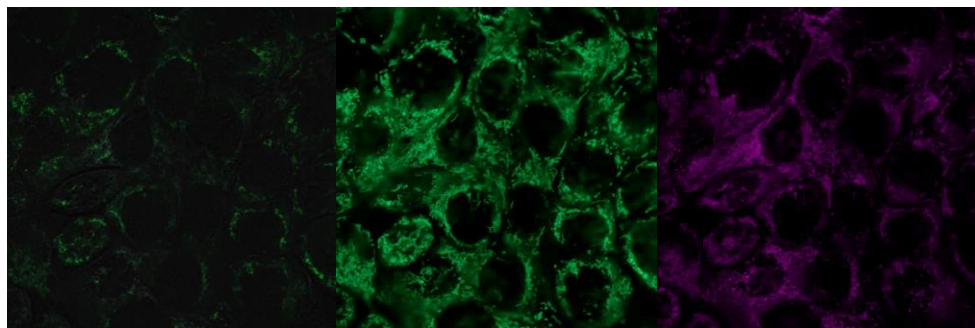
EP + WEB2086

Inactive EP + WEB2086

C.

	Merged	Mito-Bright	$^1O_2$

EP (+)

EP + DPI
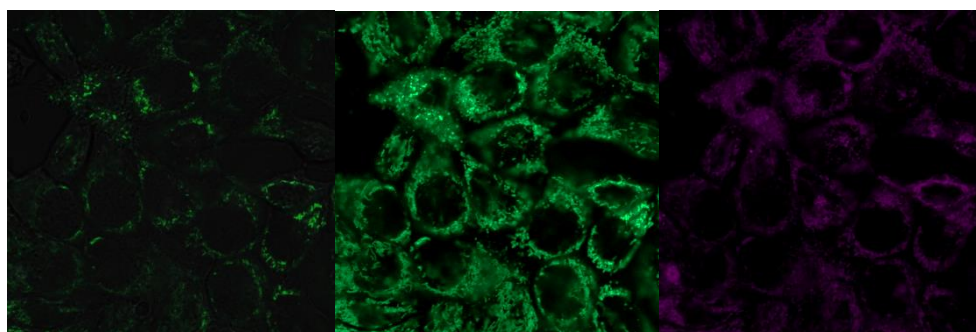
Inactive EP
+ DPI
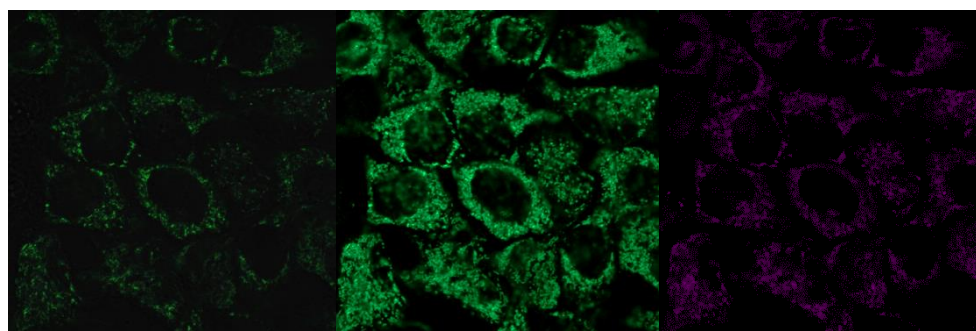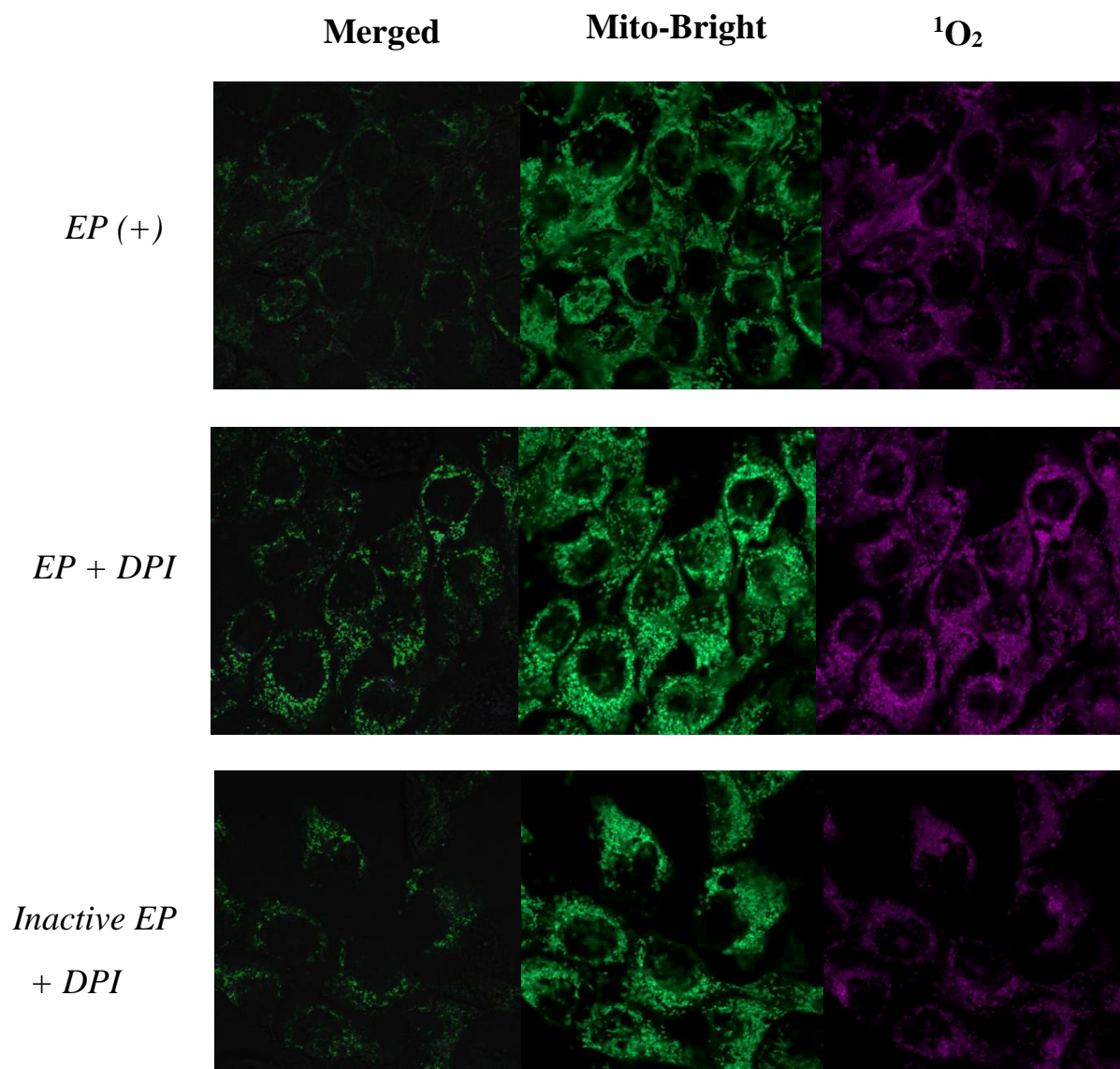
Figure 15 Si-DMA for mitochondrial $^1O_2$ imaging following 1 mM EP stimulation for 30 minutes and treatment with inhibitors/ antagonists. Cells were (A) pre-treated with the ETC inhibitors RT, AA, and TTFA at concentrations of 5 µM, 25 µM, and 250 µM respectively for 2 minutes, (B) treated with 10 µM WEB2086, (C) pre-treated with 2.5 µM DPI for 2 minutes.

A.

	Merged	**Mito-Bright**	**$^1O_2$**

EP (+)

*EP
+ MnTMPyP*

*Inactive EP
+ MnTMPyP*

B.
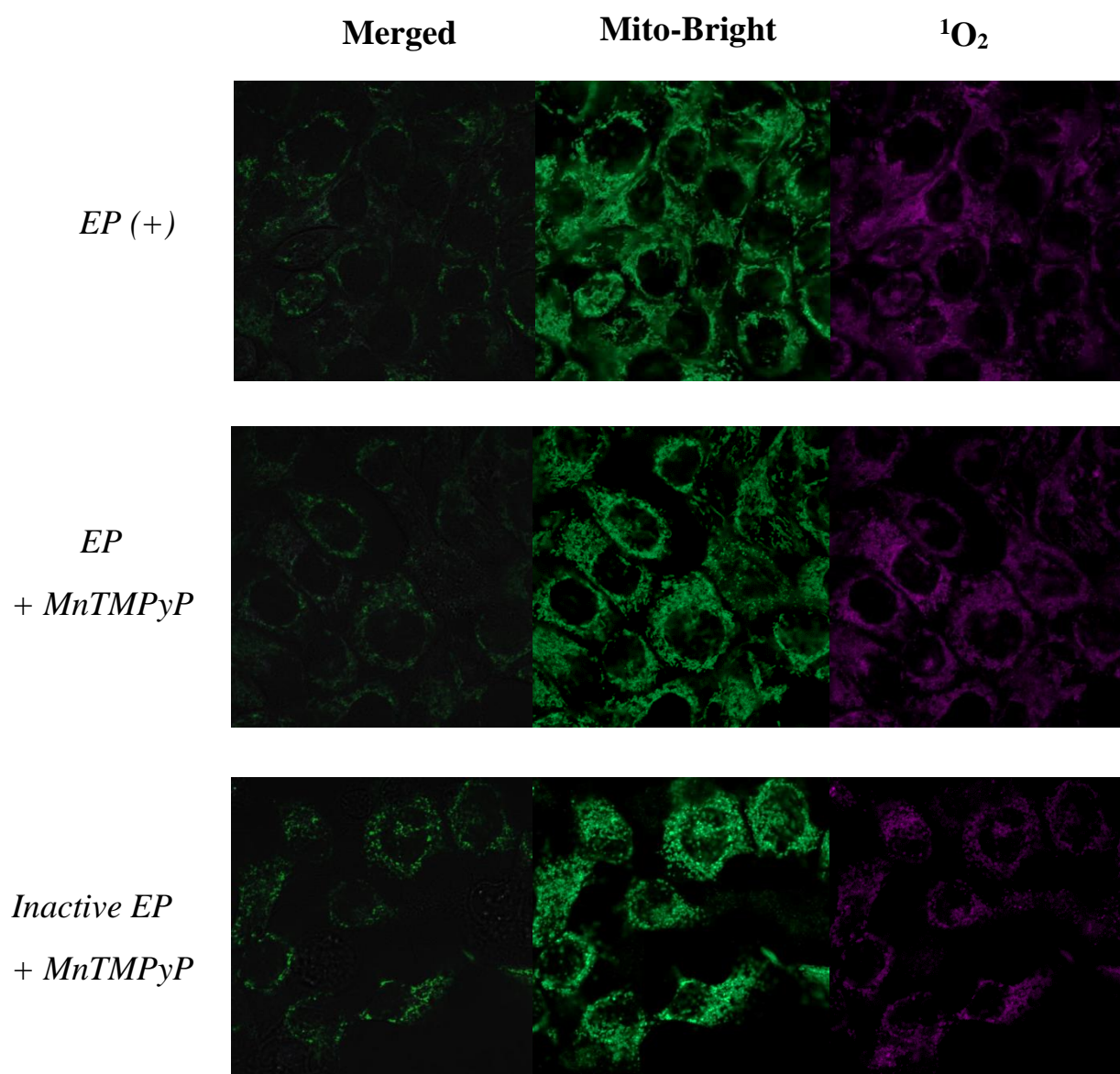
	Merged	Mito-Bright	$^1O_2$

EP (+)
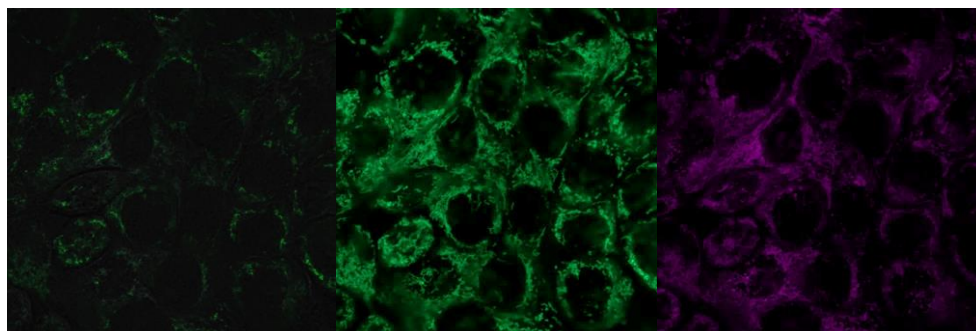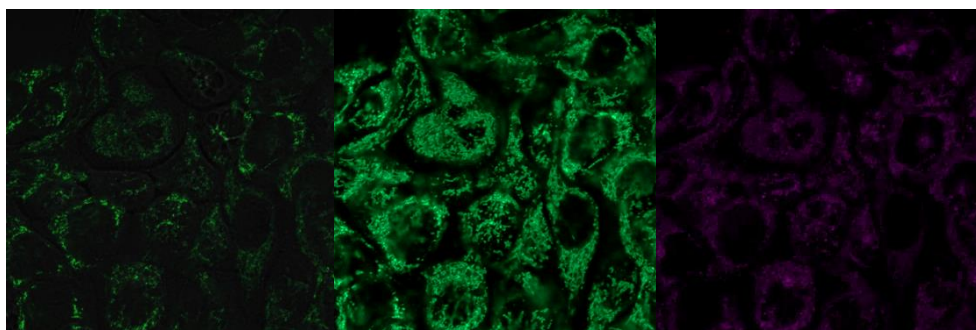
EP + NaN₃

Inactive EP + NaN₃
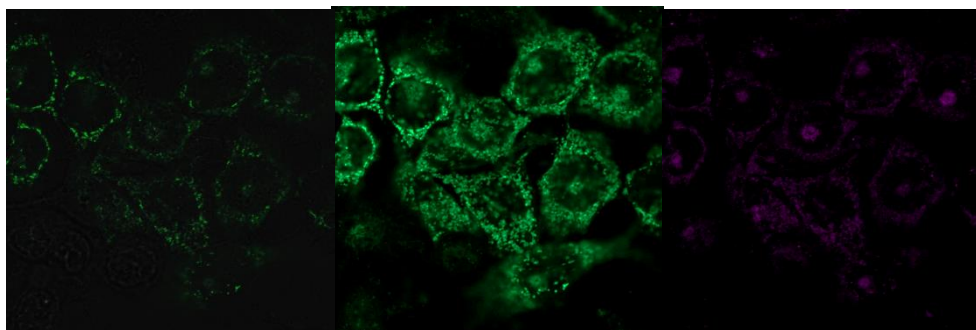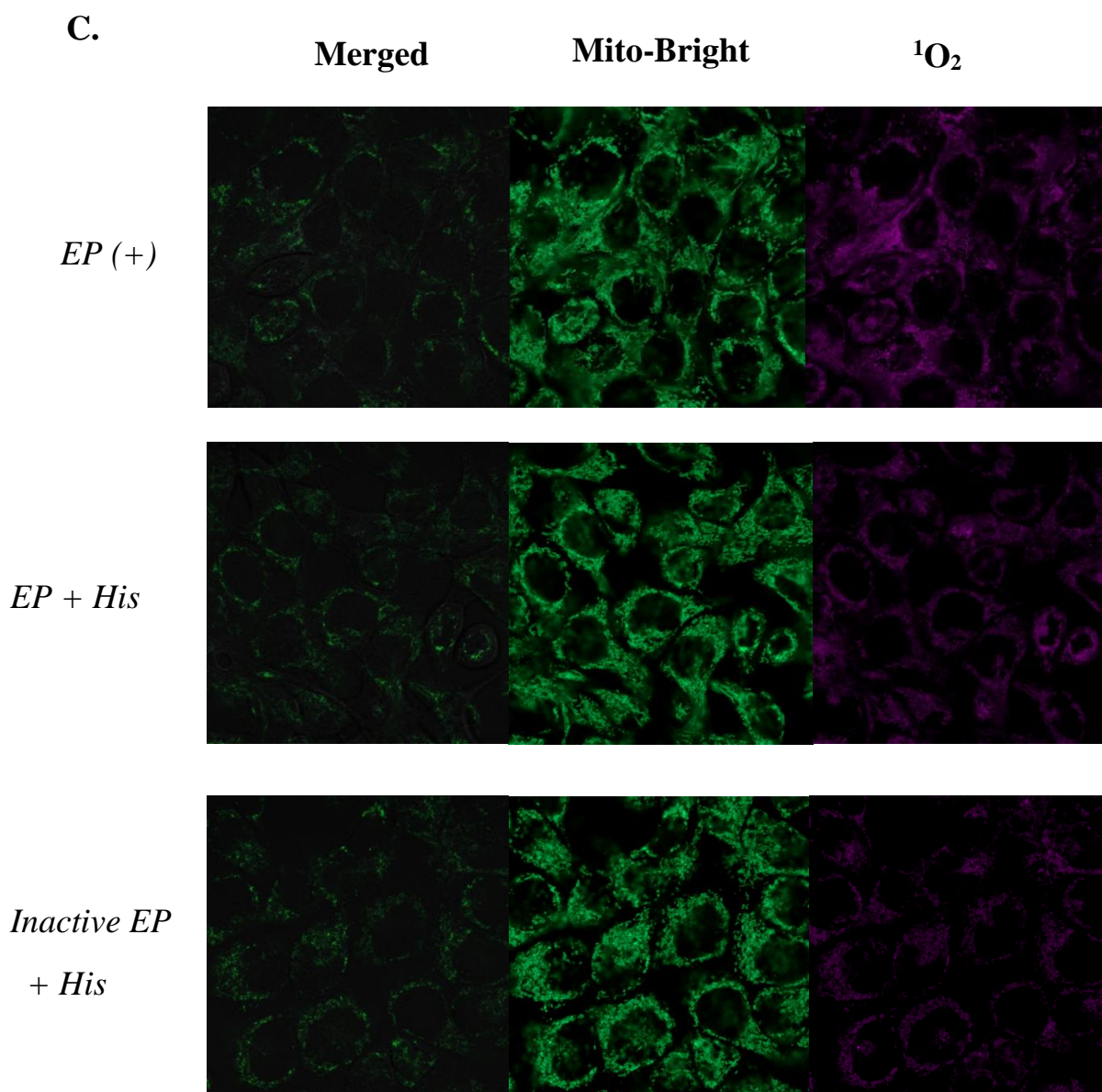
Figure 16 Si-DMA for mitochondrial $^1O_2$ imaging following 1 mM EP stimulation for 30 minutes and treatment with ROS scavengers. Cells were treated with (A) 10 μM MnTMPyP, (B) 1 mM NaN$_3$, (C) 1 mM histidine.
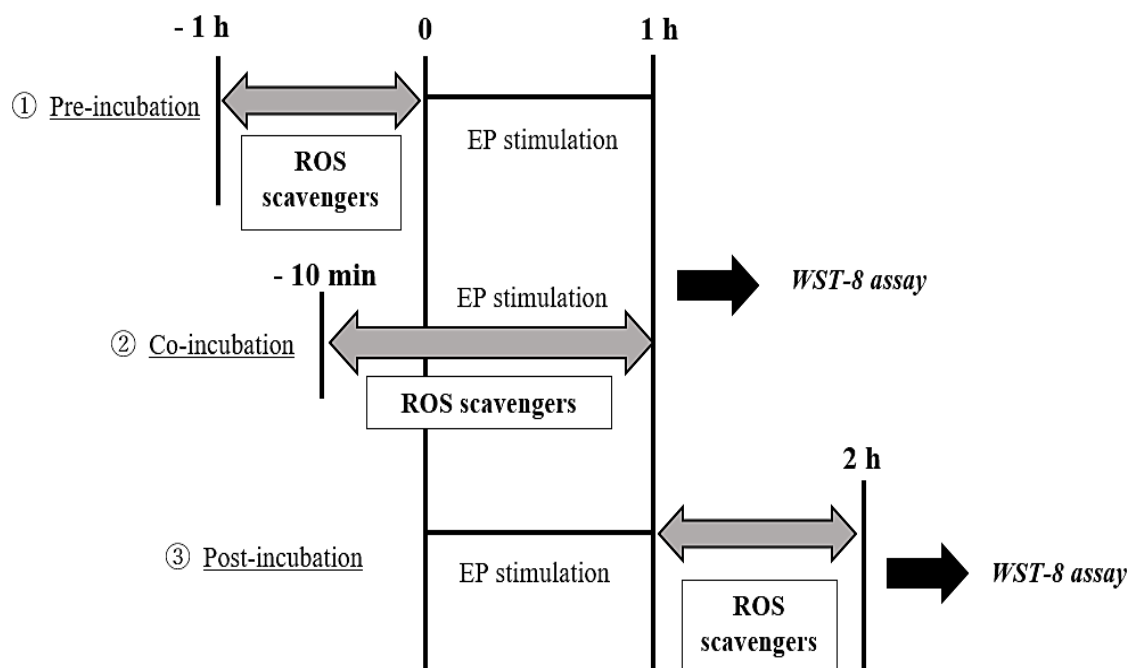
Figure 17 Experimental design for WST-8 assay with ROS scavengers and 1 mM EP stimulation. In all three tests, the cells were first seeded at a concentration of 2×10^5 in 96 well plates and incubated for 24 hours before treatment and stimulation.
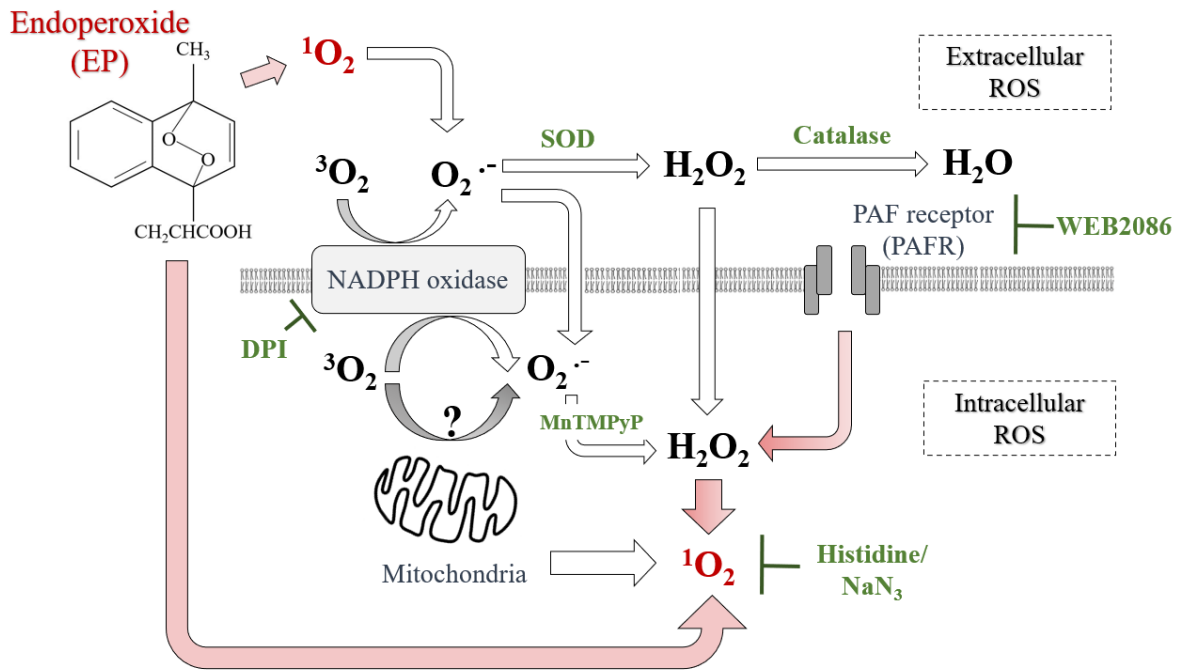
Figure 18 Hypothetical pathway for subsequent intra- and extracellular ROS production following EP stimulation.

Acknowledgments